Available online at www.sciencedirect.com

SciVerse ScienceDirect

Nuclear Physics B 873 (2013) 207–247

NUCLEAR PHYSICS B

www.elsevier.com/locate/nuclphysb

Lepton flavor violating processes $\tau \to \mu\gamma$, $\tau \to 3\mu$ and $Z \to \mu\tau$ in the supersymmetric economical 3-3-1 model

L.T. Hue *, D.T. Huong, H.N. Long

Institute of Physics, Vietnam Academy of Science and Technology, 10 Dao Tan, Ba Dinh, Hanoi, Viet Nam

Received 20 January 2013; received in revised form 21 March 2013; accepted 16 April 2013

Available online 19 April 2013

Abstract

In this work, we study the charged lepton flavor violating (cLFV) decays $\tau \to \mu\gamma$, $\tau \to 3\mu$ and $Z \to \mu\tau$ in the framework of the supersymmetric economical 3-3-1 model. Analytic formulas for branching ratios (BR) of these decays are presented. We assume that there exist lepton flavor violation (LFV) sources in both right- and left-handed slepton sectors. This leads to the strong enhancement of cLFV decay rates. We also show that the effects of the LFV source to the cLFV decay rates in the left-handed slepton sector are greater than those in the right-handed slepton sector. By numerical investigation, we show that the model under consideration contains the relative light mass spectrum of sleptons which satisfies the current experimental bounds on LFV processes in the limit of small $\tan\gamma$. The interplay between monopole and dipole operators also was studied.

Keywords: Decays of taus; Decays of Z bosons; Supersymmetric models

1. Introduction

It is known that lepton flavor (LF) numbers are strictly conversed in Standard Model (SM). However, the observation from of neutrino experiments [5] strongly suggests that there is lepton flavor mixing in lepton sector. It means that (cLFV) processes may also occur at some level. Many current experiments especially pay attention to search for LFV processes in the charged lepton sector such as tau decays [1,2], $Z \to \mu\tau$ decays [3,4], etc., because LFV observed in

* Corresponding author.
E-mail addresses: lthue@iop.vast.ac.vn (L.T. Hue), dthuong@iop.vast.ac.vn (D.T. Huong), hnlong@iop.vast.ac.vn (H.N. Long).

0550-3213/$ – see front matter
http://dx.doi.org/10.1016/j.nuclphysb.2013.04.014

experiment is evidence of new physics beyond the SM. Along with experiments, many models beyond SM that contain LFV processes have been constructed. One class of the simple extended SM models with LFV is the class of models with non-zero neutrino masses. This kind of models contains a new type of Yukawa couplings of right-handed neutrinos which are sources of cLFV. But cLFV processes in these models have been proved to be very suppressed [22,23]. However, in supersymmetric models (SUSY), the situation can be changed. Besides LFV origin affected by the new Yukawa couplings involving right-handed neutrinos, SUSY models also contain other sources of cLFV. Particularly, the large mixings of slepton mass parameters in the soft term greatly enhance the rates for cLFV processes. Because of the appearance of new cLFV sources in SUSY models, the cLFV decay rates can reach to experimental bounds even if the mixing angles in the slepton sector are small. The cLFV processes caused by this kinds of LFV were studied very early [7]. Other interesting properties supporting the study cLFV phenomenology in SUSY models were discussed in many recent works, for example [28]. Many investigations about the cLFV in SUSY models such as [10,24,9] indicated that the values of $\mathrm{BR}(\tau \to 3\mu)$ and $\mathrm{BR}(\tau \to \mu\gamma)$ may exceed the bounds of present experimental results. So it is necessary to find regions of parameter space satisfying the experimental results [2–4]:

$$\mathrm{BR}\left(\tau^- \to \mu^-\gamma\right) < 4.4 \times 10^{-8}, \tag{1}$$

$$\mathrm{BR}\left(\tau^- \to \mu^-\mu^+\mu^-\right) < 2.1 \times 10^{-8}, \tag{2}$$

$$\mathrm{BR}\left(Z \to \mu^+\tau^-\right) < 1.2 \times 10^{-5}. \tag{3}$$

Supersymmetric unified theories predict large rates for cLFV processes except the decay rate of $Z \to \mu\tau$. The branching ratio of this decay in models beyond SM is predicted to 10^{-9}–10^{-8} level [8]. It is very suppressed compared to the experimental bound (3). In fact, the GigaZ option will be approaching to the sensitivity of 10^{-8} level in the $Z \to \mu\tau$ decay mode [6]. If observed in a future experiment, it will be evidence of physics in SUSY models. One of the SUSY models in which cLFV processes are thoroughly investigated is the Minimal Supersymmetric Standard Model (MSSM) [10,11]. In the mentioned work, the authors have shown that if there exists LFV in the left-handed sector, in order to get the experimental bound on the LFV decay rates of muon and tauon decays, the mass parameters of sleptons should be shifted toward TeV scale, especially in the case of large $\tan\beta$. Because the model contains many LFV effective operators, the interplay of different effective operators (dipole, monopole coming from neutral boson exchanges and Higgs exchanges) creates many interesting consequences. The detail is discussed in works [10,11].

The current experimental results [5] show that neutrinos are massive, which contradict what assumed in the SM. Other words speaking, the SM must be extended. Among extensions, the models based on the $\mathrm{SU}(3)_C \otimes \mathrm{SU}(3)_L \otimes \mathrm{U}(1)_X$ (3-3-1) gauge group [13,14] have the following interesting features:

- To be anomaly free, the number of triplets should be equal to number of anti-triplets. This leads to that number of generations is multiple of the color number which is three. Combining with condition of the QCD asymptotic freedom the requiring number of quark generations should be less than five. Thus, in the 3-3-1 models, number of generations is three.
- The models give an explanation of electric charge quantization [15], dark matter and CP violation.
- One of the three quark families has to transform under $\mathrm{SU}(3)_L$ differently from the other two. This leads to an explanation why the top quark is uncharacteristically heavy.

The weakness of the 3-3-1 models is the complication in the Higgs sector: in the minimal 3-3-1 model [13], content of Higgs sector includes three triplets and one sextet, while in the 3-3-1 model with right-handed neutrino [14], there are three triplets. To solve the mentioned weakness, the attempt is reduction in the scalar sector. The first result is the economical 3-3-1 model [16,17] — the version with right-handed neutrino and only two Higgs triplets. Scalar sector in the minimal 3-3-1 model has been reduced to minimum with two Higgs triplets, and such version is called the reduced minimal 3-3-1 model [18]. It is emphasized that the problem on neutrino masses is not totally solved in the last version. The situation seems better in a supersymmetric version of the reduced minimal 3-3-1 model [19]. An supersymmetric version of the economical 3-3-1 model has been established in [20] and called the Supersymmetric Economical 3-3-1 model (SUSYE331). The SUSYE331 has the same advantages as its non-supersymmetric version. However, to generate masses for fermions, the non-supersymmetric models with minimal Higgs content need effective nonrenormalizable interactions, while the SUSY versions do not (the interested readers can find in Refs. [20,26]).

In [21], the LFV decays of neutral Higgs bosons in the SUSYE331 were considered. In this work, we are interested in the cLFV processes in the SUSYE331, namely: cLFV decays of the tauon and Z bosons.

We remind that in the SUSYE331, there are more leptons, Higgses and gauge bosons as well as their supersymmetric partners than those of the MSSM. This implies that the model contains many sources of LFV in the slepton sector. This suggests that the branching ratios of LFV Higgs and Z decays are greatly enhanced and may be detectable in near future. In contrast, bounds from experiments (such as shown in (1) and (2)) will strictly constrain the values of parameters causing the cLFV. So it is really important to investigate the parameter space where LVF decay rates can be satisfied the present bound of experiments. In many previous works [10,11], the authors showed that in the MSSM the interested region of parameter space is set at TeV scale with the large value of $\tan\beta$. Because of appearance of new LFV sources in the SUSYE331, we can find the interested region of parameter space even in the limit of small slepton mass parameters. In this work, we are interested in the processes: $\tau^- \to \mu^-\gamma$, $\tau^- \to \mu^-\mu^+\mu^-$ and $Z \to \mu\tau$. In particular, we incorporate the mixing of slepton mass, of charginos, Higgsino, gauginos as well as the interactions between gauge boson, slepton, lepton and the Yukawa interactions. This leads to many types of enhanced diagrams. We will consider how large contribution from each type of diagrams can be. We also will extend previous work in [10] to our considered model such as: constructing the analytical formulas of effective operators from the diagrams, from which we obtain the formulas of the branching ratios of decays $\mathrm{BR}(\tau \to \mu\gamma)$, $\mathrm{BR}(\tau \to \mu\mu\mu)$ and $\mathrm{BR}(Z \to \mu\tau)$. After that, we investigate some numerical results of these branching ratios in the limit of small $\tan\gamma$ and the slepton parameters are set below 1 TeV which may be detected by current colliders. As in the previous works on SUSYE331, $\tan\gamma$ is defined as the ratio of two vacuum expectations of two neutral Higgs components ρ and ρ', namely $\tan\gamma = \langle\rho^0\rangle/\langle\rho'^0\rangle$. Here, the quantity $\tan\gamma$ in the SUSYE331 plays a similar role as the $\tan\beta$ in the MSSM [21]. In the MSSM model, the mass of the lightest Higgs depends on $\tan\beta$ and the mass of the standard gauge bosons. If we combine the theoretical result for the upper bound on the lightest Higgs-boson mass with the direct experimental search, it leads to exclude the limit of small $\tan\beta$ for the case where soft parameters are set to TeV scale. However, this kind of constraints on the $\tan\gamma$ does not happen in the SUSYE331 model. On the other hand, the large values of $\tan\gamma$ do not support the region of the soft parameter space below 1 TeV. Hence, in this work, we concentrate on numerical studying in the limit of small $\tan\gamma$. In this paper we concentrate on only two aims. First, we establish analytic formulas to calculating some cLFV processes in the

framework of SUSYE331. Second, we prove that there exist regions satisfying the current bounds of cLFV experiments. Especially, on the basis of numerical studying, we find some interested regions of parameter space that satisfy the experimental bound on the cLFV decay rates. We also discuss on the interplay between mono and dipole operators which may lead to some interesting consequences.

This paper is arranged as follows: In Section 2 we review the particles content. The effective operators as well as branching ratios of the mentioned cLFV decay processes are presented in Section 3. Section 4 is devoted for discussion on results of numerical investigation on parameter space and the last section is the conclusion. All the analytic formulas of effective couplings appearing in effective operators and interacting terms needed for our calculation are shown in Appendices A–E.

2. Particles content

In this part, let us quickly review the particle content in the SUSYE331 model, which were given in the previous papers [20,26,21]. The fermion superfields are given by

$$\hat{L}_{aL} = \left(\hat{\nu}_a, \hat{l}_a, \hat{\nu}_a^c\right)_L^T \sim (1, 3, -1/3), \qquad \hat{l}_{aL}^c \sim (1, 1, 1), \quad a = 1, 2, 3, \tag{4}$$

$$\hat{Q}_{1L} = \left(\hat{u}_1, \hat{d}_1, \hat{u}'\right)_L^T \sim (3, 3, 1/3), \tag{5}$$

$$\hat{u}_{1L}^c, \hat{u}_L'^c \sim \left(3^*, 1, -2/3\right), \qquad \hat{d}_{1L}^c \sim \left(3^*, 1, 1/3\right), \tag{6}$$

$$\hat{Q}_{\alpha L} = \left(\hat{d}_\alpha, -\hat{u}_\alpha, \hat{d}'_\alpha\right)_L^T \sim \left(3, 3^*, 0\right), \quad \alpha = 2, 3, \tag{7}$$

$$\hat{u}_{\alpha L}^c \sim \left(3^*, 1, -2/3\right), \qquad \hat{d}_{\alpha L}^c, \hat{d}_{\alpha L}'^c \sim \left(3^*, 1, 1/3\right), \tag{8}$$

and the Higgs superfields are written as

$$\hat{\chi} = \left(\hat{\chi}_1^0, \hat{\chi}^-, \hat{\chi}_2^0\right)^T \sim (1, 3, -1/3), \qquad \hat{\rho} = \left(\hat{\rho}_1^+, \hat{\rho}^0, \hat{\rho}_2^+\right)^T \sim (1, 3, 2/3), \tag{9}$$

$$\hat{\chi}' = \left(\hat{\chi}_1'^o, \hat{\chi}'^+, \hat{\chi}_2'^o\right)^T \sim \left(1, 3^*, 1/3\right), \qquad \hat{\rho}' = \left(\hat{\rho}_1'^-, \hat{\rho}'^o, \hat{\rho}_2'^-\right)^T \sim \left(1, 3^*, -2/3\right). \tag{10}$$

It is noted that $\hat{\psi}_L^c = (\hat{\psi}_R)^c \equiv \hat{\psi}_R^\dagger$ and u', d' are exotic quarks. The values in each parenthesis show the quantum numbers of the $(\mathrm{SU}(3)_c, \mathrm{SU}(3)_L, \mathrm{U}(1)_X)$ group, respectively. The $\mathrm{SU}(3)_L \otimes \mathrm{U}(1)_X$ gauge group is broken as follows:

$$\mathrm{SU}(3)_L \otimes \mathrm{U}(1)_X \xrightarrow{w,w'} \mathrm{SU}(2)_L \otimes \mathrm{U}(1)_Y \xrightarrow{v,v',u,u'} \mathrm{U}(1)_Q, \tag{11}$$

with VEVs given by

$$\sqrt{2}\langle\chi\rangle^T = (u, 0, w), \qquad \sqrt{2}\langle\chi'\rangle^T = \left(u', 0, w'\right), \tag{12}$$

$$\sqrt{2}\langle\rho\rangle^T = (0, v, 0), \qquad \sqrt{2}\langle\rho'\rangle^T = \left(0, v', 0\right). \tag{13}$$

The SUSYE331 model contains seventeen vector superfields such as $\hat{V}_c^a$, $\hat{V}^a$ and $\hat{V}'$. The vector superfields contain the usual gauge bosons given in [20,26]. The total supersymmetric Lagrangian was given in [26]. In this work only terms relevant to our work are collected in Appendix A.

3. Effective operators and branching ratios

In this section, we extend the previous work [10] in the model under consideration. In the SUSYE331, there are six physical vector bosons: the photon, two charged ($W^{\pm}$, $Y^{\pm}$), two Hermitian neutral (Z, Z') and a non-Hermitian neutral X. The effective couplings of $X\mu\tau$ interaction is very small so we ignore them in the calculation. Let us first write down the cLFV effective operators for muon–tau and photon or Z bosons, Z' bosons or other leptons.

3.1. $\tau\mu\gamma$ effective operators

First we write down the LFV operators for τ, μ, γ. These operators are divided into two terms[1]:

$$e\big[C_L^{\gamma}\bar{\mu}\bar{\sigma}^{\mu}\tau + C_R^{\gamma}\mu^c\sigma^{\mu}\bar{\tau}^c + \text{h.c.}\big]\Box A_{\mu}, \tag{14}$$

$$em_{\tau}\big[D_L^{\gamma}\bar{\mu}\bar{\sigma}^{\mu\nu}\bar{\tau}^c + D_R^{\gamma}\mu^c\sigma^{\mu\nu}\tau + \text{h.c.}\big]F_{\mu\nu}. \tag{15}$$

The processes associated with external photon line depend only on the $D_{L,R}^{\gamma}$ while other processes with virtual photon depend on both C^{γ} and D^{γ}. The Feynman diagrams contributing to C^{γ} and D^{γ} are given in Appendix B. We would like to emphasize that the number of diagrams in the considered model is more than that of the MSSM because the SUSYE331 model contains new Higgs and gauge bosons. In order to obtain analytical formulas for C^{γ} and D^{γ}, we have used Feynman rules and some approximate expansion. For more details, the interested reader can see in Appendix B. As in the MSSM, the $C_{L(R)}^{\gamma}$ does not depend on $\tan\gamma$ and the factor $D_{L(R)}^{\gamma}$ can be divided into three sub-terms including sub-term $D_{L(R)}^{\gamma(a)}$ which is independent on $\tan\gamma$ and sub-terms $D_{L(R)}^{\gamma(c,b)}$ which are not, more specifically

$$D_{L(R)}^{\gamma} = D_{L(R)}^{\gamma(a)} + D_{L(R)}^{\gamma(b)} + D_{L(R)}^{\gamma(c)}. \tag{16}$$

We would like to mention that only $D_{L(R)}^{\gamma(c)}$ contains left–right slepton mixing parameters which, in this paper, are denoted by $(A_{\tau}, A_{\mu\tau}^{L}, A_{\mu\tau}^{R})$.

3.2. $Z\tau\mu$ and $Z'\tau\mu$ effective operator

First, let us consider the effective operator of the $Z\tau\mu$. This kind of effective operators can be written in the standard form given in [10] as follows:

$$g_Z m_Z^2\big[A_L^Z\bar{\mu}\bar{\sigma}^{\mu}\tau + A_R^Z\bar{\mu}^c\sigma^{\mu}\bar{\tau}^c + \text{h.c.}\big]Z_{\mu}, \tag{17}$$

$$g_Z\big[C_L^Z\bar{\mu}\bar{\sigma}^{\mu}\tau + C_R^Z\mu^c\sigma^{\mu}\bar{\tau}^c + \text{h.c.}\big]\Box Z_{\mu}, \tag{18}$$

$$g_Z m_{\tau}\big[D_L^Z\bar{\mu}\bar{\sigma}^{\mu\nu}\tau^c + D_R^Z\mu^c\sigma^{\mu\nu}\tau + \text{h.c.}\big]Z_{\mu\nu}, \tag{19}$$

where the mass of the Z boson in the SUSYE331 is determined as [20]:

[1] The operator containing D^{γ} is different from [10] a factor i. This is because of definition of $\sigma^{\mu\nu}$ and $\bar{\sigma}^{\mu\nu}$. The definitions in [12] are used.

$$m_Z^2 \simeq \frac{g^2(v^2+v'^2)}{4c_W^2},$$
$$g_Z \simeq \frac{g}{c_W} \quad \text{and} \quad g_{Z'} \simeq \frac{g}{\kappa_1 c_W}. \tag{20}$$

(g_Z and $g_{Z'}$ are defined from covariant derivatives, as explained in Appendices A–E.) The operators related to the factors $A^Z_{L,R}$ are chirality conserving (monopole). The leading contribution to the monopole operators comes from effective couplings of muon and tauon with two neutral Higgs bosons. In the model under consideration, we have four neutral Higgs bosons ρ^0, ρ'^0, χ_1^0 and $\chi_1'^0$ which can couple to the Z boson. However, investigation in [17] has noted the relation $u, u' \ll v, v' \ll w, w'$. In this limit, we can neglect the coupling of the Z with χ and χ'. It means that we obtain only the leading interactions of μ, τ with ρ, ρ'. These leading terms lead to a consequence that the monopole operators in (17) can be extracted out a factor m_Z^2. We would like to remind that the class of diagrams containing μ, τ, ρ^0 and ρ'^0 presented in Appendix C (Fig. 14) give contribution to $A^Z_{L,R}$ and this factor can be written as sum of three parts:

$$A^Z_{L(R)} = A^{Z(a)}_{L(R)} + A^{Z(b)}_{L(R)} + A^{Z(c)}_{L(R)}, \tag{21}$$

where analytical formulas of each term in (21) as well as $C^Z_{L(R)}$ and $D^Z_{L(R)}$ are given in Appendix C. The operator related to $C^Z_{L(R)}$ also are chirality conserving (monopole) while the operators related to $D^Z_{L(R)}$ are chirality flipping (dipole). More details about origin of these operators, the interested reader can see in [10].

A big difference compared to the MSSM is that the model under consideration contains more $\mu\tau$ effective operators such as $\mu\tau Z'$. Because of the couplings of Z' with all of neutral Higgs — χ_2^0, $\chi_2'^0$, ρ^0 and ρ'^0 — the monopole operators of $Z'\mu\tau$ relate not only to the factor m_Z^2 in but also the factor $m_{Z'}^2$, as indicated in two formulas (22) and (23). It is noted that $A^{1Z'(a)}_{L(R)}$ comes from the leading interactions of $\mu\tau$ with two neutral Higgs ρ and ρ' while the $A^{1Z'(a)}_{L(R)}$ comes from the leading interactions of $\mu\tau$ with two neutral Higgs χ_2^0 and $\chi_2'^0$. For all of others effective operators mentioned in this work — $C^{Z,(Z')}_{L,(R)}$ and $D^{Z,(Z')}_{L,(R)}$ — relate with only two neutral Higgs ρ and ρ'. Above comments are enough for us to write the standard form of $\mu\tau Z'$ operators as follows:

$$g_{Z'} m_Z^2 \big[A_L^{(1Z')} \bar{\mu}\bar{\sigma}^\mu \tau + A_R^{(1Z')} \bar{\mu}^c \sigma^\mu \bar{\tau}^c + \text{h.c.}\big] Z'_\mu, \tag{22}$$
$$g_{Z'} m_{Z'}^2 \big[A_L^{(2Z')} \bar{\mu}\bar{\sigma}^\mu \tau + A_R^{(2Z')} \bar{\mu}^c \sigma^\mu \bar{\tau}^c + \text{h.c.}\big] Z'_\mu, \tag{23}$$
$$g_{Z'} \big[C_L^{Z'} \bar{\mu}\bar{\sigma}^\mu \tau + C_R^{Z'} \mu^c \sigma^\mu \bar{\tau}^c + \text{h.c.}\big] \Box Z'_\mu, \tag{24}$$
$$g_{Z'} m_\tau \big[D_L^{Z'} \bar{\mu}\bar{\sigma}^{\mu\nu} \tau^c + D_R^{Z'} \mu^c \sigma^{\mu\nu} \tau + \text{h.c.}\big] Z'_{\mu\nu}. \tag{25}$$

Note that in the on-shell condition we have $\Box(Z) \to -m_Z^2$ and $\Box(Z') \to -m_{Z'}^2$, where:

$$m_{Z'}^2 = \frac{g^2 c_W^2 W^2}{4c_W^2 - 1}, \quad W^2 = w^2 + w'^2.$$

The $A^{1Z'}_{L(R)}$ and $A^{2Z'}_{L(R)}$ are also written in the form as those for $A^Z_{L(R)}$. Forms of the $D^Z_{L(R)}$ and $D^{Z'}_{L(R)}$ are the same of $D^\gamma_{L(R)}$ in (16). All analytical formulas of effective operators in this section are given in Appendix D.

In addition, the SUSYE331 model has two others neutral gauge bosons, Z' and X compared to the MSSM. This appearance may give significant contribution to the $\tau \to 3\mu$ decay. The mentioned contribution may be similar to that of the Z boson in some region of parameter space. This issue will be discussed in more details in the next section.

3.3. $\tau\mu\mu\mu$ effective operator

Let us write down four-fermions $\tau\mu\mu\mu$ effective operators. The $\tau\mu\mu\mu$ effective operators can be constructed from the effective operators of μ, τ with photon or Z, Z' bosons as well as Higgs bosons. Besides the contributions coming from photon, Z boson and Higgs exchanges, there are other contributions to the $\tau\mu\mu\mu$ effective operators which come from box-diagrams shown in Fig. 20. In this part, we write down only the standard form of $\tau\mu\mu\mu$ effective operator coming from box-diagrams as

$$\begin{aligned}&\big[\big(\bar{\mu}\bar{\sigma}^{\mu}\tau\big)\big(B_L^{\mu_L}\,\bar{\mu}\bar{\sigma}_{\mu}\mu + B_L^{\mu_R}\,\mu^c\sigma_{\mu}\bar{\mu}^c\big)\\&\quad + \big(\mu^c\sigma^{\mu}\bar{\tau}^c\big)\big(B_R^{\mu_L}\,\bar{\mu}\bar{\sigma}_{\mu}\mu + B_R^{\mu_R}\,\mu^c\sigma_{\mu}\bar{\mu}^c\big) + \text{h.c.}\big].\end{aligned} \tag{26}$$

Analytical forms of the coefficients $B_{L(R)}^{\mu_{L(R)}}$ are presented in Appendix E.

3.4. Branching ratios

General method to construct the branching ratios for the cLFV decay from effective operator was written in [10]. Especially, based on the basis of the effective operators, we write effective Lagrangian of the muon and tauon with photon, gauge bosons Z, Z' as well as lepton. From this effective Lagrangian, we obtain the branching ratio for each of processes by using the Feynman rules. In this section, we study the branching ratios for the considered cLFV decays of the tau and the Z bosons.

3.4.1. $\tau \to \mu\gamma$

Let us consider the cLFV decay mode $\tau \to \mu\gamma$. It is not hard to obtain the decay rate of $\tau \to \mu\gamma$ from effective operators given in Eqs. (14), (15). The detailed calculation can be seen in [24]. Comparing the branching of LFV decay $\tau \to \mu\gamma$ with that of the $\tau \to \mu\bar{\nu}_{\mu}\nu_{\tau}$ decay given in [4,12], we can obtain the relation between the two branching ratios of the two above processes. The result is entirely consistent with the results given in [10], namely

$$\text{BR}\big(\tau \to \mu^-\gamma\big) = \frac{48\pi^2\alpha}{G_F^2}\big[\big|D_L^{\gamma}\big|^2 + \big|D_R^{\gamma}\big|^2\big]\text{BR}\big(\tau \to \mu^-\bar{\nu}_{\mu}\nu_{\tau}\big), \tag{27}$$

where $\alpha = \frac{e^2}{4\pi}$, $\frac{G_F}{\sqrt{2}} = \frac{g^2}{8m_W^2}$ and $\text{BR}(\tau \to \mu^-\bar{\nu}_{\mu}\nu_{\tau}) \simeq 17.41\%$.

3.4.2. $Z \to \mu\tau$

In this subsection, we consider the decay mode of $Z \to \mu\tau$. The decay rate of $Z \to \ell^+\ell^-$ in case of the SUSY can also be determined from the general formula established in [12]. In particular, the decay rate of $Z \to \mu\tau$ in the SUSYE331 model can be written as follows:

$$\Gamma\big(Z \to \ell^+\ell^-\big) = \frac{g_Z^2 m_Z}{24\pi}\left(1 - \frac{4m_{\ell}^2}{m_Z^2}\right)^{1/2}\left[\big(a_{\ell}^2 + b_{\ell}^2\big)\left(1 - \frac{4m_{\ell}^2}{m_Z^2}\right) + 6a_{\ell}b_{\ell}\frac{m_{\ell}^2}{m_Z^2}\right], \tag{28}$$

where

$$a_\ell \equiv T_\ell^3 - Q_\ell s_W^2 = \frac{-1+2s_W^2}{2} \quad \text{and} \quad b_\ell = -Q_\ell s_W^2 = s_W^2.$$

For the decay rate of $Z \to \mu\tau$, because the form of effective operators of $Z\mu\tau$ in the considered model is the same as that of the MSSM, the form of decay rate of $Z \to \mu\tau$ is the same as that established in [10]. Especially the result is given as follows:

$$\Gamma\big(Z \to \mu^+\tau^-\big) = \frac{g_Z^2 m_Z^5}{24\pi}\left[\big|F_L^Z\big|^2 + \big|F_R^Z\big|^2 + \frac{1}{2}\left|\frac{m_\tau}{m_Z}D_L^Z\right|^2 + \frac{1}{2}\left|\frac{m_\tau}{m_Z}D_R^Z\right|^2\right], \tag{29}$$

where

$$F_{L,R}^Z = A_{L,R}^Z - C_{L,R}^Z.$$

Comparing the two results taken from Eqs. (28) and (29), we obtain the relationship between the two branching ratios corresponding to two processes $Z \to ll$ and $Z \to \mu\tau$. Our calculation is consistent with results given in [10] such as:

$$\begin{aligned}&\mathrm{BR}(Z \to \mu\tau)\\ &\quad = cm_Z^4\left[\big|F_L^Z\big|^2 + \big|F_R^Z\big|^2 + \frac{1}{2}\left|\frac{m_\tau}{m_Z}D_L^Z\right|^2 + \frac{1}{2}\left|\frac{m_\tau}{m_Z}D_R^Z\right|^2\right]\mathrm{BR}\big(Z \to \ell^+\ell^-\big),\end{aligned} \tag{30}$$

where $c \equiv (a_\ell^2 + b_\ell^2)^{-1} = (1/4 - s_W^2 + 2s_W^4)^{-1} \simeq 7.9$ and $\mathrm{BR}(Z \to \ell^+\ell^-) \simeq 3.4\%$.

3.4.3. $Z' \to \mu\tau$

Similar to the case of the Z boson, the decay rate of $Z' \to \ell^+\ell^-$ can be determined in the formula below:

$$\begin{aligned}\Gamma\big(Z' \to \ell^+\ell^-\big) &= \frac{g_{Z'}^2 m_{Z'}}{24\pi}\left(1 - \frac{4m_\ell^2}{m_{Z'}^2}\right)^{1/2}\left[\big(a_\ell'^2 + b_\ell'^2\big)\left(1 - \frac{4m_\ell^2}{m_{Z'}^2}\right) + 6a_\ell' b_\ell' \frac{m_\ell^2}{m_{Z'}^2}\right]\\ &\simeq \frac{g_{Z'}^2 m_{Z'}}{24\pi}\big(a_\ell^2 + b_\ell^2\big),\end{aligned} \tag{31}$$

where $a_\ell'^2 + b_\ell'^2 = a_\ell^2 + b_\ell^2 = 1/c$ and

$$\begin{aligned}a_\ell' &= \big(4c_W^2 - 1\big)\big(T_\ell^3 - Q_\ell\big) + 3c_W^2 X_\ell = -a_\ell,\\ b_\ell' &= -\big(4c_W^2 - 1\big)Q_{\ell_R} + 3c_W^2 X_{\ell_R} = -b_\ell.\end{aligned}$$

The decay rate $Z' \to \mu\tau$ is similar to that of $Z \to \mu\tau$. It leads to the relation between two branchings as follows:

$$\begin{aligned}\mathrm{BR}\big(Z' \to \mu\tau\big) = cm_{Z'}^4&\left[\big|F_L^{Z'}\big|^2 + \big|F_R^{Z'}\big|^2 + \frac{1}{2}\left|\frac{m_\tau}{m_{Z'}}D_L^{Z'}\right|^2 + \frac{1}{2}\left|\frac{m_\tau}{m_{Z'}}D_R^{Z'}\right|^2\right]\\ &\times \mathrm{BR}\big(Z' \to \ell^+\ell^-\big),\end{aligned} \tag{32}$$

where

$$F_{L,R}^{Z'} = \frac{m_Z^2}{m_{Z'}^2}A_{L,R}^{Z'(1)} + A_{L,R}^{Z'(2)} - C_{L,R}^{Z'}. \tag{33}$$

3.4.4. $\tau \to \mu\mu\mu$

In the SUSYE331, the effective Lagrangian described the $\tau \to \mu\mu\mu$ decay can be deduced from the effective operators given in Eq. (26) combining with those induced by the effective operators of $\mu\tau$ with Z or Z' or photon as well as Higgs boson. The general study was presented in [10]. The contributions from the box-diagrams and vector boson exchanges to the branching of the considered decay rate are sub-leading ones even when $\tan\gamma$ is large or small. However the contribution from the Higgs-bosons exchange to decay rate is large for large $\tan\gamma$ (the interested reader can see in [21]). Hence, in this work we will split each type of contributions to the considered branching ratio. First, let us consider the case of absence of Higgs exchange: the effective Lagrangian can be deduced from the effective operators given in Eqs. (15), (18), (19), (25) and (26). The explicit formula of effective Lagrangian is

$$\begin{aligned}\mathcal{L}^{\text{eff}}_{\tau\mu\mu\mu} &= \big[(\bar{\mu}\bar{\sigma}^{\mu}\tau)\big(F_L^{\mu_L}\bar{\mu}\bar{\sigma}_{\mu}\mu + F_L^{\mu_R}\mu^c\sigma_{\mu}\bar{\mu}^c\big)\\ &\quad + \big(\mu^c\sigma^{\mu}\bar{\tau}^c\big)\big(F_R^{\mu_L}\bar{\mu}\bar{\sigma}_{\mu}\mu + F_R^{\mu_R}\mu^c\sigma_{\mu}\bar{\mu}^c\big)\big]\\ &\quad + 2e^2\big(D_L^{\gamma}\bar{\mu}\bar{\sigma}^{\mu\nu}\bar{\tau}^c + D_R^{\gamma}\mu^c\sigma^{\mu\nu}\tau\big)\frac{m_{\tau}\partial_{\nu}}{\Box}\big(\bar{\mu}\bar{\sigma}_{\mu}\mu + \mu^c\sigma_{\mu}\bar{\mu}^c\big) + \text{h.c.},\end{aligned} \tag{34}$$

where

$$A^{Z'}_{L(R)} = \frac{m_Z^2}{m_{Z'}^2}A^{Z'(1)}_{L,R} + A^{Z'(2)}_{L,R}, \tag{35}$$

$$F^{\mu_L}_{L(R)} = B^{\mu_L}_{L(R)} + \frac{1}{2}g_Z^2c_{2W}A^{Z}_{L(R)} - \frac{1}{2}g_{Z'}^2c_{2W}A^{Z'}_{L(R)} - e^2C^{\gamma}_{L(R)}, \tag{36}$$

$$F^{\mu_R}_{L(R)} = B^{\mu_R}_{L(R)} + g_Z^2s_W^2A^{Z}_{L(R)} - g_{Z'}^2s_W^2A^{Z'}_{L(R)} - e^2C^{\gamma}_{L(R)}. \tag{37}$$

Here we also assume that, as in the case of MSSM, we ignore the contributions of $C^{Z}_{L,R}$, $C^{Z'}_{L,R}$, $D^{Z}_{L,R}$ and $D^{Z'}_{L,R}$ to the above effective Lagrangian. This leads to the branching ratios of decay $\tau \to \mu\mu\mu$ is

$$\begin{aligned}&\text{BR}\big(\tau^- \to \mu^-\mu^+\mu^-\big)\\ &= \frac{1}{8G_F^2}\bigg[2\big|F_L^{\mu_L}\big|^2 + \big|F_L^{\mu_R}\big|^2 + \big|F_R^{\mu_L}\big|^2 + 2\big|F_R^{\mu_R}\big|^2\\ &\quad + 4e^2\,\text{Re}\big(D_L^{\gamma}\big(2\bar{F}_L^{\mu_L} + \bar{F}_L^{\mu_R}\big) + D_R^{\gamma}\big(\bar{F}_R^{\mu_L} + 2\bar{F}_R^{\mu_R}\big)\big)\\ &\quad + 8e^2\big(\big|D_L^{\gamma}\big|^2 + \big|D_R^{\gamma}\big|^2\big)\bigg(\log\frac{m_{\tau}^2}{m_{\mu}^2} - \frac{11}{4}\bigg)\bigg]\text{BR}\big(\tau^- \to \mu^-\bar{\nu}_{\mu}\nu_{\tau}\big).\end{aligned} \tag{38}$$

3.5. $H\mu\tau$ contribution to $\tau \to \mu\mu\mu$

Contribution of Higgs exchange in the SUSYE331 model was investigated in [21], where the corresponding effective Lagrangian for this, is given by:

$$\mathcal{L}^{\text{eff}}_{\tau\mu\mu\mu} = -2\sqrt{2}G_F m_{\mu}m_{\tau}\tan\gamma\mathcal{C}\big(\mu^c\mu + \bar{\mu}\bar{\mu}^c\big)\big(\Delta_L^{\rho}\mu\tau^c + \Delta_R^{\rho}\mu^c\tau\big) + \text{h.c.}, \tag{39}$$

where

$$\mathcal{C} \equiv t_{\gamma}\bigg(\frac{s_{\alpha}^2}{m^2_{\phi_{Sa36}}} + \frac{c_{\alpha}^2}{m^2_{\varphi_{Sa36}}}\bigg). \tag{40}$$

Noting that factor $(m_\mu \tan\gamma)$ cannot be ignored if value of $\tan\gamma$ is large enough. This factor causes a shift to $F_L^{\mu_R}$ and $F_R^{\mu_L}$, explicitly

$$\delta F_L^{\mu_R} = \sqrt{2} G_F m_\mu m_\tau \mathcal{C} \Delta_R, \qquad \delta F_R^{\mu_L} = \sqrt{2} G_F m_\mu m_\tau \mathcal{C} \Delta_L. \tag{41}$$

The individual contribution from Higgs exchange to $\mathrm{BR}(\tau \to \mu^-\mu^+\mu^-)$ now is:

$$\mathrm{BR}\big(\tau \to \mu^-\mu^+\mu^-\big)_{\Phi^*} = \frac{(m_\mu m_\tau \mathcal{C})^2 (|\Delta_L^\rho|^2) + |\Delta_R^\rho|^2}{32} \mathrm{BR}\big(\tau \to \mu^- \bar{\nu}_\mu \nu_\tau\big). \tag{42}$$

This contribution will be suppressed in the case of small $\tan\gamma$. We will concentrate on this case in the numerical calculation in the following section.

4. Numerical results

In this section, let us numerically study the cLFV decays of the tau lepton $\tau \to \mu\gamma$, $\tau \to \mu\mu\mu$ and $Z \to \mu\tau$. For this purpose, we first study some constraints on values of parameter space in the SUSYE331 model.

4.1. Implication on the parameter space in SUSYE331 model

In this section, we pay attention to discussing on constraint of parameter space caused by experimental cLFV bounds (1)–(3). As mentioned, this topic has been carefully studied in many models beyond SM. Especially Ref. [10] not only indicated regions of parameter space satisfying experimental bounds but also discussed in details the correlation between dipole and non-dipole kinds of contributions to cLFV decays in each region. The most important assumption here is that sources of cLFV come from only the mass terms of sleptons in the soft term, namely only left- and right-handed slepton mass matrices have large $\mu - \tau$ entries. Let us compare the sources of cLFV appearing in the MSSM with those of the SUSYE331. Because of the absence of the right-handed neutrinos, the MSSM contains only three sources of cLFV, particularly LFV in left-handed charged sleptons, left-handed sneutrinos and right-handed charged leptons. But the left-handed sleptons and their sneutrinos live in the same doublet of $\mathrm{SU}(2)_L$ in the MSSM, the origin of cLFV in the left-handed charged sleptons and left-handed sneutrinos sectors are the same. As a consequence, in the MSSM there are only two independent sources of cLFV. Due to the appearance of the right-handed neutrinos in the SUSYE331, there also appears one more source of LFV. Furthermore, there exist two Higgs multiplets in the model, i.e., triplet ρ and anti-triplet ρ' which independently generate masses of charged and neutral sleptons at tree level. These two Higgs multiplets also create at least two new corresponding mass terms of sleptons in the soft term, as shown in details in [20,26,21]. In general, there are at least four independent sources causing the cLFV in the SUSYE331 where each source is parameterized by a mixing angle defined in the last subsection of Appendix A. This parameterization creates the similarity between the SUSYE331 and the MSSM. We exploit this advantage to make some prediction for the SUSYE331 basing previous investigation of the MSSM. For example, if all of these sources are appeared, the branching ratio of decay $\tau \to \mu\gamma$ will be much enhanced than that in the MSSM, even it could greatly exceed the bound of experiment given in (1). As considered in the MSSM, the existence of maximal LFV mixing in the left-handed slepton sector means the LFV mixing in both charged and neutral sleptons, and their contributions to cLFV decays are much larger than contributions caused by right-handed LFV mixing. In addition, if the superparticle spectrum is relative light, namely the parameter space are set below 1 TeV, there will exist

very small regions of parameter space satisfying experimental results. The similar situation also happens for the SUSYE331. However, in the SUSYE331 four cLFV sources are independent then there exists a situation that the model contains only one left-handed maximal LFV source while others vanish. It is easy to realize that in this case, the values of branching ratios of cLFV processes in the SUSYE331 are smaller than those of the MSSM and the satisfied regions of parameter space will be wider in the scale of $\mathcal{O}(100)$ GeV. On the other hand, if four LFV sources are presented, the predicted results of the considered model consistent with the experimental results at the TeV scale. In the next subsections, we will examine the influence of LFV sources appearing in the soft term of the SUSYE331 on the cLFV decays of the tau and the Z boson. In the numerical investigation, we just pay attention to the case of soft parameters at $\mathcal{O}(100)$ GeV scale because this scale allows the existence of small values of slepton masses which can be detected by present colliders. In fact, the detailed investigation to determine different properties of cLFV branching ratios among different regions of parameter space is really needed, as done in many known SUSY models. In the SUSYE331, this work is more complicated because of the addition of many new particles so we will come back this interesting topic in another work.

We would like to emphasize that the sleptons gain mass through main sources which come from soft terms and interacting terms of sleptons with Higgs through F- and D-terms. As mentioned in [27], the D-term gives contribution to mass of slepton that contribution is proportional to the quantity $(w^2 - w'^2)$ while F-term gives contribution to mass of slepton that is proportional to $(\lambda_a w)$ or $(\lambda_a w')$. Because the VEVs ω and ω' break down $\mathrm{SU}(3)_L$ to $\mathrm{SU}(2)_L$ so these values can be set to the TeV scale. We would like to note that the SUSYE331 contains the Tachyon fields, the removal Tachyon fields leads to a condition [26]:

$$\left|w^2 - w'^2\right| \simeq \left|v^2 - v'^2\right| \leqslant 246^2 \left(\mathrm{GeV}^2\right). \tag{43}$$

However, in the last work [26], we have ignored the B-type terms, namely $B_\rho \rho\rho'$, $B_\chi \chi\chi'$. If the B-type terms are included into the Higgs potential, not only the tachyon fields are removed without any conditions but also the stable vacuums are guaranteed. From now, we will consider the SUSYE331 which include the above B-terms. It is noted that the Higgs mass spectrum is different from that presented in [20,26]. For example, there are three neutral massive pseudoscalar, five neutral massive scalar and four charged massive Higgs. It is interesting that masses of light Higgs, in general, increase by the presence of B-type terms. Especially, the charged Higgs mass of m_W^2 as shown in [26] now changes into the new value of $(m_W^2 + 2B_\rho/\sin 2\gamma)$. So the B-terms will make masses of Higgs satisfied with current limits of electroweak precision tests such as LEP limit of charged Higgs boson [30], even without loop corrections. For more detail, the interested reader can see in Refs. [29,31]. In the SUSYE331, where the B-type terms are included, the D-term generates mass for slepton at the $\mathrm{SU}(3)_L$ scale by sub-terms which are always proportional to $(w^2(t_\beta^2 - 1)/t_\beta^2)$ [27]. So this contribution should be at the $\mathcal{O}(100)$ GeV if slepton masses are in range of $\mathcal{O}(100)$ GeV. This is similar to the condition (43). Furthermore, if the R-parity is imposed, the coupling λ_a must vanish. It means that the contributions from both F- and D-terms to masses of sleptons depend on the $\mathrm{SU}(3)_L$ broken scale and the value of t_β. So if both slepton masses are in the range of $\mathcal{O}(1)$ TeV scale and t_β is close to unity, the dominant contribution to the slepton masses comes from the soft term.

Next, let us discuss on μ_ρ and μ_χ which play the same role as μ parameter in the MSSM. According to [20,26], including B-type terms, the requirement of canceling all linear terms at tree level in the Higgs potential leads to conditions:

$$\mu_\chi^2 + 4m_\chi^2 - 4\frac{B_\chi}{t_\beta} = \frac{g^2}{1-4c_{2W}}\left[2c_{2W}\left(\frac{t_\beta^2-1}{t_\beta^2}\right)(w^2+u^2) + \left(\frac{t_\gamma^2-1}{t_\gamma^2}\right)v^2\right],$$

$$\mu_\rho^2 + 4m_\rho^2 - 4\frac{B\rho}{t_\beta} = \frac{g^2}{1-4c_{2W}}\left[\left(\frac{t_\beta^2-1}{t_\beta^2}\right)(w^2+u^2) - 2\left(\frac{t_\gamma^2-1}{t_\gamma^2}\right)v^2\right],$$

$$m_\chi^2 + m_\chi'^2 + \frac{\mu_\chi^2}{2} = B_\chi\frac{t_\beta^2+1}{t_\beta},$$

$$m_\rho^2 + m_\rho'^2 + \frac{\mu_\rho^2}{2} = B_\rho\frac{t_\gamma^2+1}{t_\gamma}. \tag{44}$$

The parameters $\mu_\chi^2, \mu_\rho^2, m_\chi^2$ and m_ρ^2 as well as $m_{\rho'}^2, m_{\chi'}^2$ are positive. The additional B-terms depend on the phases of fields. We can redefine the phases of χ, χ', ρ and ρ' by such way that can absorb any phase in the B-terms, so we can take B_χ, B_ρ to be real and positive. The conditions given in Eqs. (44) lead to the consequences as follows: The scale of all parameters given in the left-handed side of Eqs. (44) are the same order. If the value of $\tan\beta$ is closed to the unit, the parameters μ_χ^2, μ_ρ^2, m_χ^2, m_ρ^2, $m_{\rho'}^2$, $m_{\chi'}^2$ and B_χ, B_ρ are set to the scale of electroweak symmetry breaking else they are set to the scale of $SU(3)_L$ symmetry breaking. Furthermore the Higgs mass spectrum studied in [31] also leads to the conclusions on the limit of $\tan\gamma$. Specially if the soft and μ/B parameters given in Higgs potential are considered at the scale of $SU(3)_L$ symmetry breaking the tree level mass of the SM Higgs boson is $m_Z|\cos 2\gamma| < 92.0$ GeV. This result is similar to that given in the MSSM. In this case, the boundary of the SM mass can be pushed up to 130 GeV by one-loop correction with large $\tan\gamma$. In another case if the soft μ/B-terms are considered at the scale of electroweak symmetry breaking, there is no constraint on the value of $\tan\gamma$.

It is known that three branching ratios $\tau \to \mu\gamma$, $\tau \to \mu\mu\mu$ and $Z \to \mu\tau$ depend on some of following quantities: $A_{L(R)}^{Z(Z')}$, $B_{L(R)}^{\mu_{L(R)}}$, $C_{L(R)}^{\gamma(Z,Z')}$ and $D_{L,R}^{\gamma(Z,Z')}$. In different regions of parameter space, where some of these quantities give dominant contribution, there are precise correlations among branching ratios. In particular, with three considering branching ratios, we have two cases as listed below:

D^γ-dominance: It is easy to get the relation concerned in [10]

$$\frac{\mathrm{BR}(\tau \to \mu\mu\mu)}{\mathrm{BR}(\tau \to \mu\gamma)} \simeq 2.2 \times 10^{-3}, \tag{45}$$

and a consequence is

$$\mathrm{BR}(\tau \to \mu\mu\mu) < 10^{-10}. \tag{46}$$

A^Z-dominance: In this case, we get

$$\mathrm{BR}(\tau \to \mu\mu\mu) = \begin{pmatrix} 0.53 \\ 0.67 \end{pmatrix} \mathrm{BR}(Z \to \mu\tau). \tag{47}$$

Note that in the SUSYE331 model, although $A_{L(R)}^{Z'}$ receives contribution from diagrams which are similar to those of $A_{L(R)}^{Z}$, $A_R^{Z'} \simeq 0$. In the limit $t_\beta = \omega/\omega' \simeq 1$ ($c_{2\beta} = 0$) and $A_L^{Z'}$ depends on only diagrams containing right-handed sneutrinos.

In next subsection, we consider numerical computation for cLFV decays of the tauon and the Z boson. Remember that the effective couplings used for numerical studying are established in Appendices B, C, D and E. The standard loop integrals are given in [10,25]. In the following investigation, we use most of the notations defined in [21]. For example, mass parameters of gauginos and Higgsinos are listed in the formula (B.2): m_λ denotes mass of $SU(3)_L$ gaugino, μ_ρ and μ_χ are μ-terms of Higgsinos. Only notation for mass of U(1) gaugino used in this work is m_B instead of m'.

4.2. *In the case of small* $\tan\gamma$ *and light mass spectrum*

4.2.1. $\tau \to \mu\gamma$

Let us consider the numerical studying of branching of $\tau \to \mu\gamma$ decay. The analytical result given in Eq. (27) depends on the effective coupling $D^\gamma_{L(R)}$ which can be divided into three parts, $D^\gamma_{L(R)} = D^{\gamma(a)}_{L(R)} + D^{\gamma(b)}_{L(R)} + D^{\gamma(c)}_{L(R)}$. The analytical formulas of $D^{\gamma(a)}_{L(R)}$, $D^{\gamma(b)}_{L(R)}$ and $D^{\gamma(c)}_{L(R)}$ are given in Appendix B in which only $D^{\gamma(a)}_{L(R)}$ does not depend on $\tan\gamma$. In addition, from the experimental bound (1), we can obtain the constraint on the effective couplings, namely $|D^\gamma_{L,R}| \leqslant 2.5 \times 10^{-9}$ [GeV^{-2}].

We would like to remind that the diagrams which contribute to the D^γ_L are collected from three LFV sources: left-handed charged slepton, left-handed sneutrinos and right-handed sneutrinos sectors, while the diagrams contributing to D^γ_R are only collected from the charged right-handed slepton sector. So the values of D^γ_L are predicted much larger than those of D^γ_R. Another thing we want to emphasize that since the SUSYE331 has many additional particles, we expected that the additional particles can modify the predicted results of cLFV decay in the model under consideration. For more details, let us consider numerical studying in this decay mode.

First we study the effects of LFV sources on D^γ_L in the case of small $\tan\gamma$ as well as the presence of all of the three left-handed LFV sources, especially we fix $\tan\gamma = 3$ and $\theta_L = \theta_{\tilde{\nu}_L} = \theta_{\tilde{\nu}_R} = \pi/4$. As in the MSSM, $D^{\gamma(b)}_L$ is dominant contribution to D^γ_L. Fig. 1 shows the dependence of $D^{\gamma(b)}_L$ on soft parameters $m_{\tilde{L}_3} = m_{\tilde{\nu}_{L_3}} = m_{\tilde{\nu}_{R_3}}$ and m_λ, while other parameters are fixed. The predicted results given in left panel of Fig. 1 are fully consistent with the experimental results if the domain of parameter m_{L3} is close to the value of $m_{\tilde{L}2}$ and all soft parameters are set at $\mathcal{O}(100)$ GeV. We also remind that mixing mass term between left and right slepton, $m_{\tilde{\psi}_{\mu\tau}}$, is small if the model under consideration has maximal mixing sources. However if μ_ρ is set at TeV, the domain of parameter $m_{\tilde{L}2}$, where the values of $D^{\gamma(b)}_L$ match experimental bound, is more extensive. For more details, the reader can see in the right panel of Fig. 1.

Let us consider the case $m_{\tilde{L}3} = 1$ TeV. The results given in Fig. 2 predict that the values of $D^{\gamma(b)}_L$ exceed the experimental bound if the remaining parameters are assumed in region of $\mathcal{O}(100)$ GeV. Even if the values of μ_ρ are assumed as large as 1 TeV, the predicted value of $D^{\gamma(b)}_L$ is larger than the experimental bound. In this region of parameter space, the predicted results in the SUSYE331 are much similar to those in the MSSM [10]. As mentioned in [10], the large values of A_τ as well as small values of μ_ρ and masses of sleptons must be required to keep value of the total $|D^\gamma|$ below the experimental bound. However, Fig. 2 displays that the predicted values of $D^{\gamma b}_L$ are much greater than those in the MSSM. It means that in order to obtain the values of $D^{\gamma(b)}_L$ being consistent with experimental bound, the values of A_τ predicted in the SUSYE331 should be much larger than those in the MSSM. In the limit of large values of A_τ, the

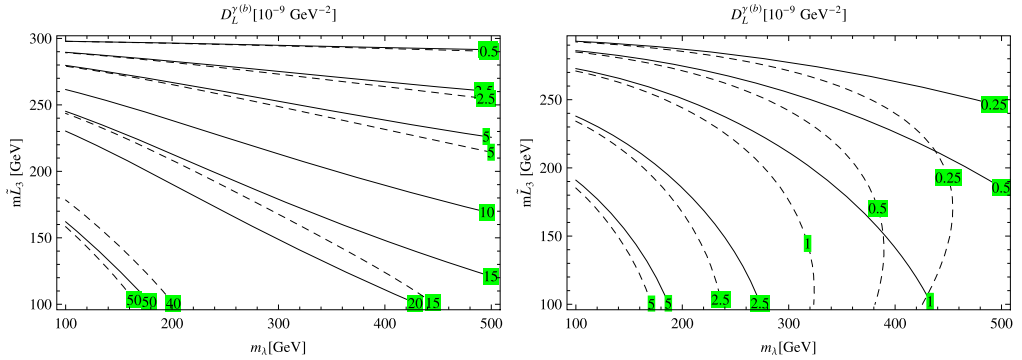

Fig. 1. $D_L^{\gamma(b)}$ isocontours with $\tan\gamma = 3$, $m_{\tilde{L}_3} = m_{\tilde{\nu}_{L_3}} = m_{\tilde{\nu}_{R_3}}$ and $m_{\tilde{L}_2} = m_{\tilde{\nu}_{L_2}} = m_{\tilde{\nu}_{R_2}} = 300$ GeV, $\theta_L = \theta_{\tilde{\nu}_L} = \theta_{\tilde{\nu}_R} = \pi/4$ and $\mu_\rho = 140$ GeV (1 TeV) in the left (right) panel. The solid and dashed lines correspond to $m_B = 300$ GeV and $m_B = -300$ GeV.

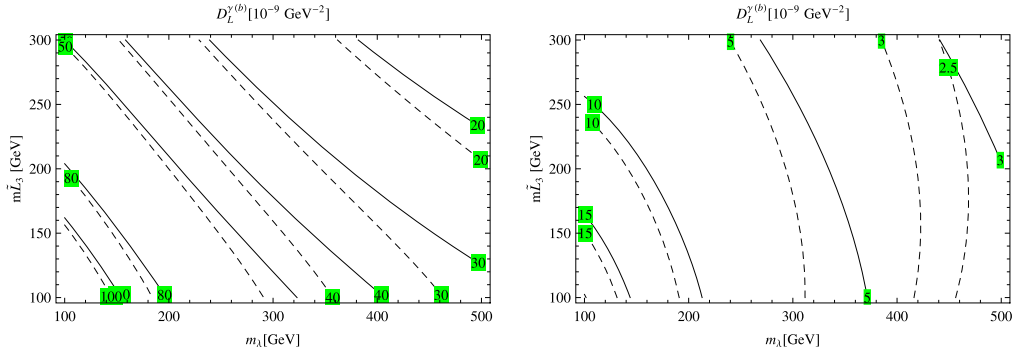

Fig. 2. $D_L^{\gamma(b)}$ isocontours with $\tan\gamma = 3$, $m_{\tilde{L}_2} = m_{\tilde{\nu}_{L_2}} = m_{\tilde{\nu}_{R_2}}$ and $m_{\tilde{L}_2} = m_{\tilde{\nu}_{L_2}} = m_{\tilde{\nu}_{R_2}} = 1$ TeV, $\theta_L = \theta_{\tilde{\nu}_L} = \theta_{\tilde{\nu}_R} = \pi/4$ and $\mu_\rho = 140$ GeV (1 TeV) in the left (right) panel. The solid and dashed lines correspond to $m_B = 300$ GeV and $m_B = -300$ GeV.

model leads to the appearance of Tachyon sleptons. It means that the model under consideration does not contain the region of parameter space such that there exists a large difference between the values of slepton masses. Fig. 2 also shows that the values of $D_L^{\gamma(b)}$ exceed to the experimental results when parameter $m_{\tilde{L}}$ expands into range of TeV.

So in the SUSYE331 model with the case of the maximal mixing happening in all three sources (left-handed slepton, left-handed sneutrino and right-handed sneutrino sectors), the scale of all slepton masses should be the same order, in range of TeV or in range of (100) GeV.

Now we consider another situation that happens only in the SUSYE331, not in the MSSM. It is the case of only one left-handed LFV source appearing in the model. Looking at analytical formulas of effective couplings, three sources contributing to left-handed effective coupling are parameterized by three mixing angels θ_L, $\theta_{\tilde{\nu}_L}$ and $\theta_{\tilde{\nu}_R}$. Two of them, $\theta_{\tilde{\nu}_L}$ and $\theta_{\tilde{\nu}_R}$, relate with diagrams containing sneutrino propagators while the remain relates to diagrams with charged slepton propagators. Numerical computation indicates that if the mass spectrum of superpartner particles is in the range of $\mathcal{O}(100)$ GeV, contribution from sneutrino exchanges are larger than those of charged slepton ones. So if two sneutrino mixing angles vanish, there is only

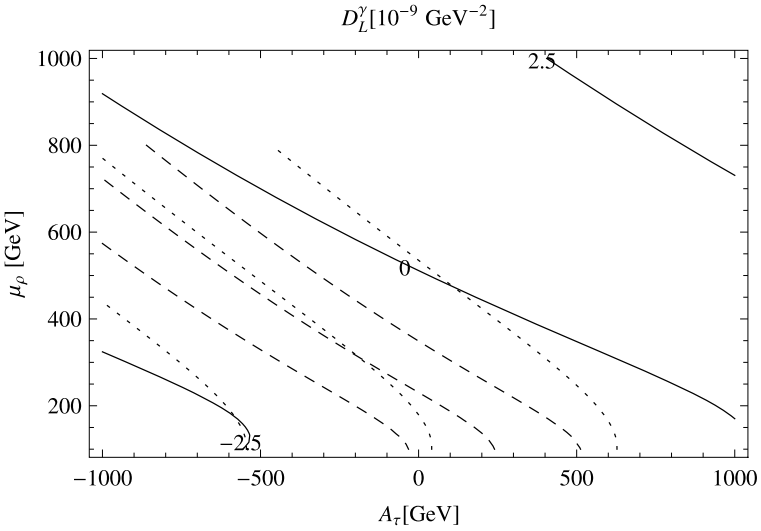

Fig. 3. D_L^γ isocontours with $\tan\gamma = 3$, $m_{\tilde{L}_2} = 1$ TeV, $\theta_L = \pi/4$, $\theta_R = \theta_{\tilde{\nu}_L} = \theta_{\tilde{\nu}_R} = 0$, $A^L_{\tau\mu} = 0$ (only LFV in $\{\tilde{m}_L, \tilde{\tau}_L\}$ sector). For illustrations, we choose three choices of parameter space $(m_B, m_\lambda, m_{\tilde{L}_3}, m_{\tilde{R}})$ in GeV: (200, 300, 300, 200) (solid), (100, 400, 100, 200) (dashed), (100, 500, 300, 100) (dotted). For each example, the center line corresponds to the value of $D_L^\gamma = 0$, two other ones limit the region where $|D_L^\gamma| \leqslant 2.5 \times 10^{-9}$ [GeV^{-2}].

one source of left-handed mixing θ_L which generates relatively small effective couplings. The experimental bounds then are easily satisfied even in regions of light mass spectrum. Our numerical investigation will focus on this case. In particular, mixing angle parameters are fixed as $\theta_R = \theta_{\tilde{\nu}_L} = \theta_{\tilde{\nu}_R} = 0$ and $\theta_L = \pi/4$. Fig. 3 displays $D_L^{\gamma b}$ as function of the A_τ and μ_ρ while others are fixed: $m_{\tilde{L}2} = 1$ TeV, $m_{\tilde{R}_2} = m_{\tilde{R}_3} = m_{\tilde{\nu}_{L_2}} = m_{\tilde{\nu}_{L_3}} = m_{\tilde{\nu}_{R_2}} = m_{\tilde{\nu}_{R_3}} \equiv m_{\tilde{R}}$. The results given in Fig. 3 illustrate that in the considered limit, we can find the region of the small absolute values of A_τ in which we can obtain the values of $|D_L^\gamma|$ satisfying the experimental bound, particularly:

- The value of m_B should be smaller than that of m_λ.
- If the value of m_B is closer to that of m_λ, the parameter space of A_τ and, μ_ρ satisfying the experimental bound of $|D_L^\gamma|$ has been expanded.

The predicted results given in Fig. 3 show that if in the SUSYE331, only one source of lepton number violation in the charged slepton sector, the model can contain the region of parameter space in which the all soft parameters are set to $\mathcal{O}(100)$ GeV except $m_{\tilde{L}_2}$ is set to TeV. In this region of parameter space, the predicted results on the $\tau \to \mu\gamma$ are matched the experimental bound on the decay. The existence of the soft parameter space below TeV scale leads to hope that the sleptons can be detected by LHC.

Finally, we consider the LFV effect in the right-handed charged slepton sector to the LFV in the tauon decay. We assume that there is only the maximal mixing of right-handed slepton, i.e., $s_R = c_R = 1/\sqrt{2}$ and all other mixing sources are set to be equal to zero. Under this assumption the Feynman diagrams in the model under consideration contributing to D^γ are exactly the same as those in the MSSM [10]. In Fig. 4, absolute values of $D_R^{\gamma(a)}$ and $D_R^{\gamma(b)}$ are rather small, even a bit smaller than those in the MSSM. From this investigation, we see that A_τ should have the same order with the mass parameters of sleptons.

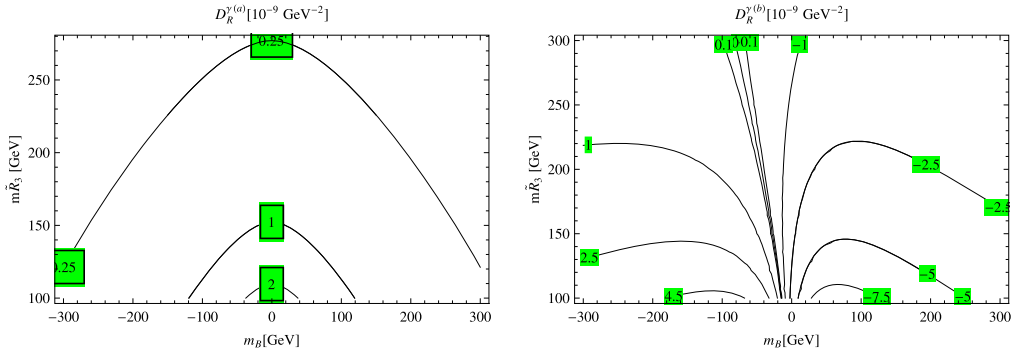

Fig. 4. Isocontours of $D_R^{\gamma(a)}$ (left panel) and isocontours of $D_R^{\gamma(b)}$ (right panel). The parameters are $\tan\gamma = 3$, $m_{\tilde{R}_2} = 1$ TeV, $\theta_L = \theta_{\tilde{\nu}_L} = \theta_{\tilde{\nu}_R} = 0$, $\theta_R = \pi/4$ and $\mu_\rho = 150$ GeV.

4.2.2. Correlations

Next, we consider the process $\tau \to \mu\mu\mu$. The amplitude consists of the contributions from the effective couplings $A_{L(R)}, B_{L(R)}, C_{L(R)}$ and $D_{L(R)}$ which are denoted the coupling of Z, Z' gauge bosons, photon and Higgs to charged leptons $\mu_{L(R)}, \tau_{L(R)}$. Each type of diagrams picking up the each particle exchange contributing to the LFV in the considered process depends on the region of parameter space. In next work, we will study the contribution of each effective coupling to the LFV of the $\tau \to \mu\mu\mu$ process in two typical cases.

Only maximal mixing in the charged slepton $(\tilde{\mu}, \tilde{\tau})$.

Let us consider the process $\tau \to \mu\mu\mu$ in the limit of small $\tan\gamma$ and in the case of existing only maximal mixing in the charged slepton, $s_L = c_L = \frac{1}{\sqrt{2}}$ and $s_R = s_{\tilde{\nu}_L} = s_{\tilde{\nu}_R} = 0$. This constraint leads to $A_L^{2Z'} = A_R^{2Z'} = 0$. As mentioned in the last part, it is interesting to consider the region of parameter at $\mathcal{O}(100)$ [GeV]. One can check that $A_{L(R)}^Z$ is dominated by $A_{L(R)}^{Z(a)}$ and total effective couplings contributing to the branching ratio of the considered process are $D_{L(R)}^\gamma$, $C_{L(R)}^\gamma$, $A_L^{Z(a)}$ and $B_L^{\mu_{L(R)}}$. Indeed, looking at the analytical expression of these couplings we found that only the analytical expression of D_L^γ is affected by left-handed slepton parameters such as: A_τ, $A_{\mu\tau}^L$. Hence, in order to look for the effective coupling giving dominant contribution to the considered branching ratio, we will study numerically two cases:

- The A_τ, $A_{\mu\tau}$ parameters are fixed and the other soft parameters are changed.
- The soft parameters are fixed and the A_τ, $A_{\mu\tau}$ parameters are changed.

First, we assume that $A_\tau = A_{\mu\tau} = 0$. To assess the contribution of the each effective coupling A_L^Z and D_L^γ into the $\mathrm{BR}(\tau^- \to \mu^-\mu^+\mu^-)$, we define two factors f_{AZ} and f_{D^γ} such as:

$$f_{AZ} \equiv \frac{g_Z^4[|A_L^Z|^2(\frac{1}{2}c_{2W}^2 + s_W^4) + |A_R^Z|^2(\frac{1}{4}c_{2W}^2 + 2s_W^4)]}{2|F_L^{\mu_L}|^2 + |F_L^{\mu_R}|^2 + |F_R^{\mu_L}|^2 + 2|F_R^{\mu_R}|^2} \tag{48}$$

and

$$f_{D^\gamma} \equiv \frac{8e^4(|D_L^\gamma|^2 + |D_R^\gamma|^2)[\ln(\frac{m_\tau^2}{m_\mu^2}) - \frac{11}{4}]}{MS} \tag{49}$$

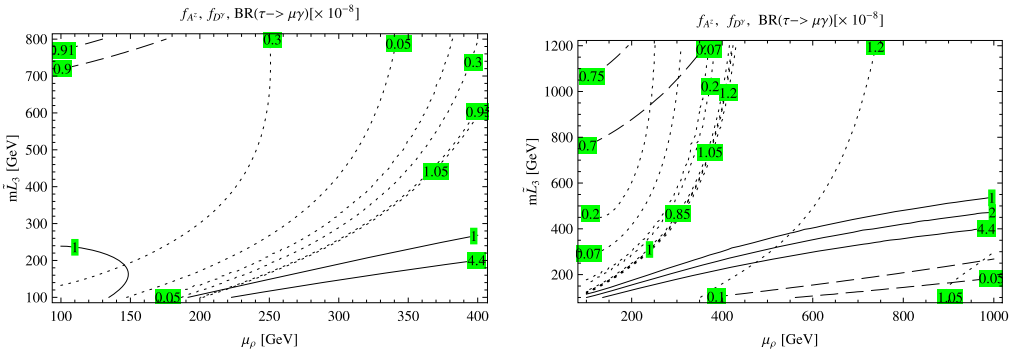

Fig. 5. Correlations among A_L^Z, $F_L^{\mu_{L(R)}}$ and D_L^γ with $A_\tau = 0$. The contours $f_{A_L^Z}$, $f_{D_L^\gamma}$ and $\mathrm{BR}(\tau \to \mu\gamma)$ are denoted by dashed, dotted and solid black lines. For illustrations, numerical values for parameter space $(m_B, m_\lambda, m_{\tilde{L}_2}, m_{\tilde{R}})$ are chosen as (100, 300, 1000, 100) [GeV] (left panel) and (100, 500, 1000, 100) [GeV] (right panel).

where

$$MS = 8e^4\left(\left|D_L^\gamma\right|^2 + \left|D_R^\gamma\right|^2\right)\left[\ln\left(\frac{m_\tau^2}{m_\mu^2}\right) - \frac{11}{4}\right] + 2\left|F_L^{\mu_L}\right|^2 + \left|F_L^{\mu_R}\right|^2 + \left|F_R^{\mu_L}\right|^2 + 2\left|F_R^{\mu_R}\right|^2. \tag{50}$$

The factors f_{A^Z} and f_{D^γ} given in Eqs. (48), (49) quantitatively measure contributions of $A_{L(R)}^Z$ and $D_{L(R)}^\gamma$ to the factor $|F^{\mu_{L(R)}}|$ and the total branching of $(\tau^- \to \mu^-\mu^+\mu^-)$ decay, respectively.

Looking at Eqs. (36) and (37), the coefficient $F_{L(R)}^{\mu_{L(R)}}$ depends on the other factors. If A^Z gives dominant contribution to $F_{L(R)}^{\mu_{L(R)}}$, it is convenient to define regions where the factor f_{A^Z} satisfies $1.05 \geqslant f_{A^Z} \geqslant 0.95$ as the A^Z-domination regions (over $F_{L(R)}^{\mu_{L(R)}}$). On the other hand, we also make convention that if $f_{D^\gamma} \leqslant 0.05$ then the dominant contribution to the branching ratio of $\tau \to 3\mu$ is given by F-type of couplings and if $1.05 \geqslant f_{D^\gamma} \geqslant 0.95$ then the dominant contribution to the branching ratio of $\tau \to 3\mu$ is given by D-type of couplings.

The current experimental upper bound on the branching ratio of the process $\mathrm{BR}(\tau \to \mu\gamma)$ is smaller than 4.4×10^{-8}. The results of our calculation to this process is given in Fig. 5. The experimental bound of the branching is denoted by the solid black lines. One can see that this process satisfies the experimental bound in regions of large parameter space of μ and $m_{\tilde{L}_3}$.

The regions of parameter space where A_L^Z gives dominant contribution to branching ratio $\tau \to 3\mu$ must satisfy both conditions: $1.05 \geqslant |f_{A^Z}| \geqslant 0.95$ and $|f_{D^\gamma}| \leqslant 0.05$. The results given in Fig. 5 show that there is no region of μ_ρ and $m_{\tilde{L}_2}$ parameter space that make A_L^Z given dominant contribution to branching ratio $\tau \to 3\mu$. If D^γ gives dominant contribution to the considered decay mode, the region of the μ_ρ parameter satisfied the condition $1.05 \geqslant |f_{D^\gamma}| \geqslant 0.95$, strongly depends on the value of charged gaugino mass, i.e., if the charged gaugino mass is larger, then the value of μ_ρ parameter is larger too.

Let us consider the effects of A_τ on the branching of the considered decay mode. We would like to emphasize that A^Z does not depend on the A_τ while the value of $|D_L^\gamma|$ depends on the sign as well as amplitude of A_τ. In particularly $D_L^{\gamma(c)}$ is proportional to $(A_\tau + \frac{1}{2}\mu_\rho \tan\gamma)$, the values of A_τ will affect on soft parameter space region where D_L^γ gives dominant contribution to the $\mathrm{BR}(\tau \to 3\mu)$. These regions of soft parameter can be larger than that in the case of $A_\tau = 0$.

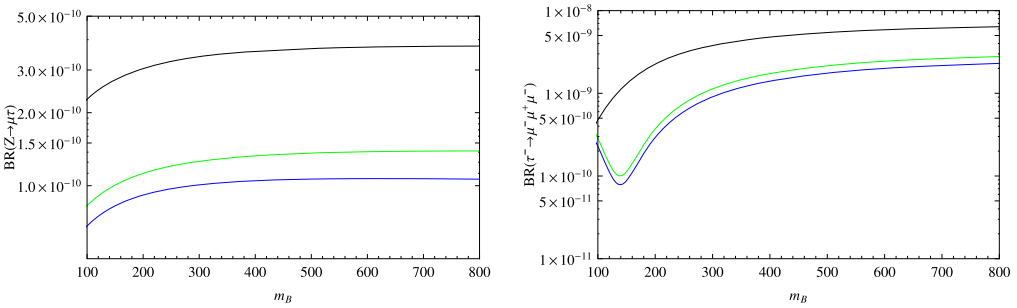

Fig. 6. Branching ratios $Z \to \mu\tau$ (left panel) and $\tau \to 3\mu$ (right panel) as functions of m_B. Three numerical values for parameter space $(m_\lambda, \mu_\rho, m_{\tilde{L}_2}, m_{\tilde{L}_3}, m_{\tilde{R}})$ [GeV] are chosen: (300, 150, 1000, 100, 100) — black line, (400, 200, 1000, 100, 100) — green line, (500, 150, 1000, 100, 100) — blue line. (For interpretation of the references to color in this figure legend, the reader is referred to the web version of this article.)

Now let us consider $Z \to \mu\tau$ and $\tau \to \mu\mu\mu$ decays. The branching ratios of decays $Z \to \mu\tau$ and $\tau^- \to \mu\mu\mu$ are presented in (29) and (47). The predicted branching is shown in Fig. 6. The numerical branching ratio for $Z \to \mu\tau$ has the maximum of 5×10^{-10} if the soft parameters of sleptons are set to $\mathcal{O}(100)$ GeV and the charged gaugino mass is set to few hundreds GeV. This predicted result is very suppressed with the present experimental bound. However, in the same region of soft parameter space, the predicted result for $\tau \to \mu\mu\mu$ can reach to the experimental result and even one can find some regions of parameter space that predicted our result exceed the experimental bound. One can check in the left panel of Fig. 6, the branching values for $Z \to \mu\tau$ hardly change when we change the value of the parameter m_B. However, the situation is quite different if the charged gaugino mass is varied, namely the smaller value of charged gaugino mass is, the larger value of that branching is predicted. Moreover, as we increase the values of the soft slepton mass parameters these branching values decreased. Therefore, to increase the value of the branching of $Z \to \mu\tau$, we have to change the parameter μ_ρ.

Fig. 7 shows the values of branching ratios of the decays in the plane m_B–μ_ρ. In this case, we choose $A_\tau = 0$ and other parameters are chosen so that the experimental branching decay of $\mathrm{BR}(\tau \to \mu\mu\mu)$ is satisfied. We can see that the bounded regions of $\mathrm{BR}(\tau \to \mu\gamma)$ supports the small values of both remain decays. In the case $A_\tau \neq 0$, because only $\mathrm{BR}(\tau \to \mu\gamma)$ depends on the values of A_τ and as we have shown in the above section, there will exist a possibility where D_L^γ vanishes. This case allows $\mathrm{BR}(\tau^- \to \mu^-\mu^+\mu^-)$ can reach the limits of experiment of order $\mathcal{O}(10^{-8})$ whilst $\mathrm{BR}(Z \to \mu\tau)$ is still in maximal order of $\mathcal{O}(10^{-9})$.

Only maximal mixing in the right-handed charged slepton sector $\tilde{\mu}, \tilde{\tau}$.

Now we come to consider another case, only maximal LFV in right-handed sector of charged sleptons ($s_R = 1/\sqrt{2}$, $s_L = s_{\tilde{\nu}_L} = s_{\tilde{\nu}_R} = 0$) where regions of parameter space can be available in range of $\mathcal{O}(100)$ [GeV]. Both the SUSYE331 and the MSSM models are similar to each other in this case. So we just discuss more on correlation among effective couplings. As shown in the left panel of Fig. 8, the bound of experiment of $\mathrm{BR}(\tau \to \mu\gamma)$ rules out the large values of $\mathrm{BR}(\tau \to 3\mu)$. This leads to the result $\mathrm{BR}(\tau \to 3\mu) \leqslant 10^{-9}$ if $A_\tau = 0$. The right panel shows that in the case of only large LFV in right-handed charged slepton sector, the $\mathrm{BR}(\tau \to 3\mu)$ is in maximal order of 10^{-9}, even in the case of non-vanishing A_τ and A_τ makes D_R^γ suppressed. For the $\mathrm{BR}(Z \to \mu\tau)$, this case is much smaller than the previous case. Also we can see a difference from

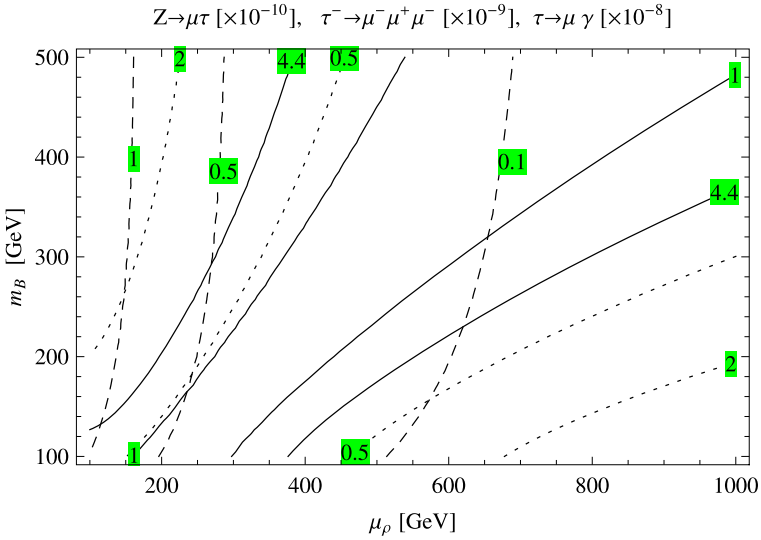

Fig. 7. Contour plots for branching ratios $\tau^- \to \mu^-\mu^+\mu^-$ (dotted), $Z \to \mu\tau$ (dashed) and $\tau \to \mu\gamma$ (solid) with $A_\tau = 0$ and $(m_\lambda, m_{\tilde{L}_2}, m_{\tilde{L}_3}, m_{\tilde{R}}) = (400, 150, 1000, 100, 200)$.

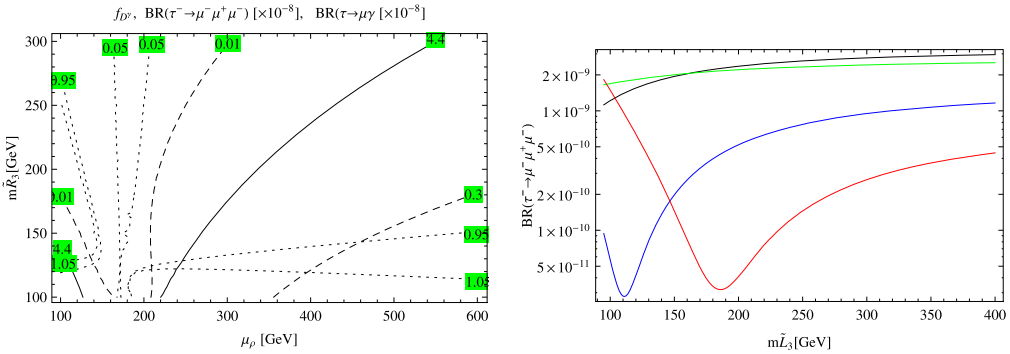

Fig. 8. Contours in μ_ρ–$m_{\tilde{R}_3}$ plane (left panel) and plots of branching ratio of $\tau \to 3\mu$ (right panel) in the case of $\tan\gamma = 3$ and $A_\tau = 0$. The respective contours are $\mathrm{BR}(\tau \to \mu\gamma)$ (solid lines), f_{D^γ} (dotted lines) and $\mathrm{BR}(\tau \to 3\mu)$ (dashed lines) with numerical values of parameters $(m_B, m_{\tilde{L}}, m_{\tilde{R}_2}) = (100, 100, 1000)$ $(m_{\tilde{L}_2} = m_{\tilde{L}_3} \equiv m_{\tilde{L}})$. For the plot of $\mathrm{BR}(\tau \to 3\mu)$ four choices of parameter space $(m_B, \mu_\rho, m_{\tilde{R}_2}, m_{\tilde{R}_3})$ are: (100, 100, 1000, 100) (black), (200, 100, 1000, 100) (green), (100, 200, 1000, 100) (blue) and (100, 300, 1000, 100) (red). (For interpretation of the references to color in this figure legend, the reader is referred to the web version of this article.)

the case of pure large LFV in left-handed charged slepton sector: the D^γ-domination regions now lie on the small values of μ_ρ while the large values of μ_ρ are ruled out by the condition $\mathrm{BR}(\tau \to \mu\gamma) \leqslant 4.4 \times 10^{-8}$.

5. Conclusions

In present paper, we have studied the LFV decays of the tauon and the Z boson in framework of the SUSYE331 model, and have mainly focused on two-generations slepton mixing, namely

both left- and right-handed $\tilde{\mu}$–$\tilde{\tau}$ slepton mixings. In order to obtain the relevant diagrams, we have combined the mixing of sleptons, that of charginos, Higgsinos, gauginos as well as the interactions of gauge bosons with leptons and the Yukawa interactions. From these diagrams, we obtained the effective operators relating to the considered cLFV decays. This leads to the analytical expression of the branching ratio of the considered decay processes and the contacted relation between decay rate of non-LFV decay mode with that of cLFV decay mode. Our analysis is carried out in the limit of small $\tan\gamma$. The detailed predictions in our model depend strongly on the SUSY parameters and left- and right-handed slepton mixing. Consequently, we have firstly considered the effects of SUSY parameters and the mixing of left- and right-handed sleptons on the $\tau \to \mu\gamma$ decay such as

- In the case of the maximal LFV mixing, the mixing mass terms between left- and right-handed sleptons ($m_{\tilde{L}_{\mu\tau}}, m_{\tilde{R}_{\mu\tau}}$) are small, our results are only consistent with the experimental bounds if the domains of parameter $m_{\tilde{L}_3}$ are close to those of $m_{\tilde{L}_2}$ whenever they are set to the TeV or $\mathcal{O}(100)$ GeV scales. It means that in the case of maximal LFV mixing, the slepton mass parameters are in the same order.
- If there is only the LFV in the charged left-handed slepton sector, we can find some regions of parameter space that allow above cLFV branching ratios matching with the experimental bounds. Especially the slepton mass $m_{\tilde{L}_3}$ is set at 1 TeV while the other, $m_{\tilde{L}_2}$, is set at $\mathcal{O}(100)$ GeV. Noting that the value of parameter m_B should be close to that of m_λ and if the value of m_B is closer to that of m_λ, the parameter space of A_τ has been more expanded. In the case of left-handed LFV sector, one important result deduced from our numerical investigation is that although the SUSYE331 model contains much more supersymmetric particles as well as LFV sources than the MSSM, there still exist of some wide regions of parameter space which allow not only masses of sleptons but also μ_ρ keep the small values enough to be detected by colliders.
- If there is only the LFV in the charged right-handed slepton sector, in order to match the experimental bound, the value of A_τ should be the same order as that of other soft parameters. Our result is similar to the predicted result in the MSSM.

Based on the parameter space satisfying the experimental bound on $\tau \to \mu\gamma$ decay rate, we consider the branching ratios of $\tau \to \mu\mu\mu$ and $Z \to \mu\tau$. We have concentrated on the LFV in the charged left-handed slepton sector with only $\theta_L = \pi/4$. In this case, there is no region of parameter space that A_Z gives dominant contribution to the considered decay mode, while there is region of parameter space that D^γ gives dominant contribution to the considered decay mode. The constraint on the μ parameter is expanded toward large values if the large value of the charged gaugino mass is chosen. If we set the value of $A_\tau = 0$, the constraint on the μ parameter can be expanded. Similarly, by numerical study on the branching ratio of $\tau \to \mu\mu\mu$ decay mode in the case there exists LFV only in the charged right-handed slepton sector. The small value of μ_ρ giving the dominant contribution to considered decay mode coming from D^γ was obtained. In both cases, our predicted results of $\mathrm{BR}(Z \to \mu\gamma)$ are very suppressed.

Acknowledgements

L.T. Hue would like to thank Dr. A. Brignole for the explanation of the establishing analytical formulas in [10]. This research is funded by Vietnam National Foundation for Science and Technology Development (NAFOSTED) under grant No. 103.01-2011.63.

Appendix A. Interacting Lagrangian and notations

Some of the interacting vertices used in this work were given in [21]. In this appendix we list the rest part of interacting Lagrangian which is necessary for completion our calculation. Here we use the relation $\tilde{\ell}_R \equiv (\tilde{\ell}^c_L)^*$ where $\tilde{\ell}^c_L$ is the superpartner of a lepton ℓ^c_L in the model.

A.1. Interaction between left–right slepton sector with neutral Higgs boson

These terms come from two sources:

(1) from F-terms:

$$-\frac{1}{2}\left[\mu_\rho \rho^0 \left(Y_\mu \tilde{\mu}^*_L \tilde{\mu}^{c*}_L + Y_\tau \tilde{\tau}^*_L \tilde{\tau}^{c*}_L\right) + \text{h.c.}\right],$$

(2) from soft-breaking term:

$$\begin{aligned}
\mathcal{L}^{\text{soft}}_{\tilde{l}\tilde{l}H^0} &= -h'_{ab}\tilde{L}_{aL}\rho'\tilde{l}^c_{bL} + \text{h.c.} \\
&= -h'_{ab}\left(\tilde{\nu}_{aL}\rho'^-_1 + \tilde{l}_{aL}\rho'^0 + \tilde{\nu}^c_{aL}\rho'^-_2\right)\tilde{l}^c_{bL} + \text{h.c.} \\
&\to -Y_\mu A_\mu \rho'^0 \tilde{\mu}_L \tilde{\mu}^c_L - Y_\tau A_\tau \rho'^0 \tilde{\tau}_L \tilde{\tau}^c_L \\
&\quad - Y_\tau A^L_{\mu\tau} \rho'^0 \tilde{\mu}_L \tilde{\tau}^c_L - Y_\tau A^R_{\mu\tau} \rho'^0 \tilde{\tau}_L \tilde{\mu}^c_L + \text{h.c.},
\end{aligned} \tag{A.1}$$

where we use new notations that are identified with those in [10]:

$$\begin{aligned}
h'_{22} &= h'_{\mu\mu} \equiv Y_\mu A_\mu, \qquad & h'_{33} &= h'_{\tau\tau} \equiv Y_\tau A_\tau, \\
h'_{23} &= h'_{\mu\tau} \equiv Y_\tau A^L_{\mu\tau}, \qquad & h'_{32} &= h'_{\tau\mu} \equiv Y_\tau A^R_{\mu\tau}.
\end{aligned}$$

The total interaction part of $(H^0 \tilde{l}^c_L \tilde{l}_L)$ interactions is:

$$\begin{aligned}
\mathcal{L}^{LR}_{\tilde{l}\tilde{l}H^0} = &-Y_\mu \left(\frac{1}{2}\mu_\rho \rho^{0*} + A_\mu \rho'^0\right)\tilde{\mu}_L \tilde{\mu}^c_L - Y_\tau \left(\frac{1}{2}\mu_\rho \rho^{0*} + A_\tau \rho'^0\right)\tilde{\tau}_L \tilde{\tau}^c_L \\
&- Y_\tau A^L_{\mu\tau} \rho'^0 \tilde{\mu}_L \tilde{\tau}^c_L - Y_\tau A^R_{\mu\tau} \rho'^0 \tilde{\tau}_L \tilde{\mu}^c_L + \text{h.c.}
\end{aligned} \tag{A.2}$$

A.2. Gauge boson interactions

This kind of vertex is only contained in gauge invariant kinetics of all fields in the theory. In this work, we just study on cLFV in lepton sector so the related part of the Lagrangian is [20]:

$$\begin{aligned}
\mathcal{L}_{\text{kinetic}} = &\left(D^\mu \rho\right)^\dagger D_\mu \rho + \left(\bar{D}^\mu \rho'\right)^\dagger \bar{D}_\mu \rho' + i\bar{\tilde{\rho}}\bar{\sigma}^\mu D_\mu \tilde{\rho} + i\bar{\tilde{\rho}}'\bar{\sigma}^\mu \bar{D}_\mu \tilde{\rho}' \\
&+ \left(D^\mu \tilde{L}_{iL}\right)^\dagger D_\mu \tilde{L}_{iL} + i\bar{L}_{iL}\bar{\sigma}^\mu D_\mu L_{iL} \\
&+ \left(D_{1\mu} l^c_{iL}\right)^\dagger D_{1\mu} l^c_{iL} + i\bar{l}^c_{iL}\bar{\sigma}^\mu D_{1\mu} l^c_{iL} \\
&- \frac{1}{4}F^{\mu\nu}_a F_{a,\mu\nu} - \frac{1}{4}F^{\mu\nu}F_{\mu\nu} + i\bar{\lambda}^a_V \bar{\sigma}^\mu D^L_\mu \lambda^a_V + i\bar{\lambda}_B \bar{\sigma}^\mu \partial_\mu \lambda_B
\end{aligned} \tag{A.3}$$

where $i = 1, 2, 3$ is family index, $a = 1, 2, \ldots, 8$ corresponds to eight gauge bosons of $\text{SU}(3)_L$ group. Covariant derivatives D_μ, $\bar{D}_\mu$, $D_{1\mu}$ and D^L_μ correspond to triplets, anti-triplets $\text{SU}(3)_L$, singlet $\text{SU}(3)_L$ and adjoint presentation of $\text{SU}(3)_L$. They are defined as follows:

$$
\begin{aligned}
&F_{a\mu\nu} = \partial_\mu V_{a\nu} - \partial_\nu V_{a\mu} - g f^{abc} V_{b\mu} V_{c\nu}, \qquad F_{\mu\nu} = \partial_\mu B_\nu - \partial_\nu B_\mu,\\
&D_\mu = \partial_\mu + igT^a V_{a\mu} + ig' X T^9 B_\mu,\\
&\bar{D}_\mu = \partial_\mu - igT^{a*} V_{a\mu} + ig' X T^9 B_\mu,\\
&D_{1\mu} = \partial_\mu + ig' X T^9 B_\mu,\\
&D^L_\mu \lambda^a_V = \partial_\mu \lambda^a_V - g f^{abc} V^b \lambda^c_V.
\end{aligned} \tag{A.4}
$$

Here X denotes U(1) hypercharge, f^{abc} is structure constant of SU(3), T^9 is the generator of $U(1)_X$ which is defined by $T^9 = 1/\sqrt{6}\,\mathrm{diagonal}(1,1,1)$. We just pay attention to neutral bosons in covariant derivatives so they can be written as [20,17].

$$
\begin{aligned}
D^N_\mu &\equiv \partial_\mu + i\mathcal{P}^{\mathrm{NC}}_\mu\\
&= \partial_\mu + ig\big(T^3 V_{3\mu} + T^8 V_{8\mu} + tT^9 X B_\mu + T^4 V_{4\mu} + T^5 V_{5\mu}\big),\\
\bar{D}^N_\mu &\equiv \partial_\mu - i\mathcal{P}^{\mathrm{NC}}_\mu\\
&= \partial_\mu - ig\big(T^3 V_{3\mu} + T^8 V_{8\mu} - tT^9 X B_\mu\big) - ig\big(T^4 V_{4\mu} - T^5 V_{5\mu}\big),\\
D_{1\mu} &= \partial_\mu + ig' X T^9 B_\mu,\\
D^L_\mu \lambda^a_V &= \partial_\mu \lambda^a_V - g\big(f^{a3c} V^3_\mu + f^{a8c} V^8_\mu + f^{a4c} V^4_\mu + f^{a5c} V^5_\mu\big)\lambda^c_V,
\end{aligned} \tag{A.5}
$$

where gauge bosons W_3, W_8, W_4, and B relate with physical states according to the transformation:

$$
\begin{pmatrix} W_3\\ W_8\\ B\\ W_4 \end{pmatrix} =
\begin{pmatrix}
s_W & c_\varphi c_{\theta'} c_W & s_\varphi c_{\theta'} c_W & s_{\theta'} c_W\\
-\frac{s_W}{\sqrt{3}} & \frac{c_\varphi \kappa_3 - s_\varphi \kappa_1 \kappa_2}{\sqrt{3} c_W c_{\theta'}} & \frac{s_\varphi \kappa_3 + c_\varphi \kappa_1 \kappa_2}{\sqrt{3} c_W c_{\theta'}} & \sqrt{3} s_{\theta'} c_W\\
\frac{\kappa_1}{\sqrt{3}} & -\frac{t_W (c_\varphi \kappa_1 + s_\varphi \kappa_2)}{\sqrt{3} c_{\theta'}} & -\frac{t_W (s_\varphi \kappa_1 - c_\varphi \kappa_2)}{\sqrt{3} c_{\theta'}} & 0\\
0 & -t_{\theta'}(c_\varphi \kappa_2 - s_\varphi \kappa_1) & -t_{\theta'}(s_\varphi \kappa_2 + c_\varphi \kappa_1) & \kappa_2
\end{pmatrix}
\begin{pmatrix} A\\ Z\\ Z'\\ W'_4 \end{pmatrix},
\tag{A.6}
$$

where some new notations are used:

$$
\begin{aligned}
&t_\theta \equiv \tan\theta = \frac{u}{w}, \qquad t_{2\theta} \equiv \tan(2\theta), \qquad s_{\theta'} = \frac{t_{2\theta}}{c_W \sqrt{1 + 4t^2_{2\theta}}},\\
&t \equiv \frac{g'}{g} = \frac{3\sqrt{2} s_W}{\sqrt{3 - 4s^2_W}}, \qquad \kappa_1 \equiv \sqrt{4c^2_W - 1} = \frac{3\sqrt{2} s_W}{t},\\
&\kappa_2 \equiv \sqrt{1 - 4s^2_{\theta'} c^2_W}, \qquad \kappa_3 = s^2_W - 3c^2_W s^2_{\theta'}.
\end{aligned} \tag{A.7}
$$

In the SUSYE331 model, we have all θ, φ and $\theta' \ll 1$. Thus, we can use the approximation $\sin\theta = \sin\varphi = \sin\theta' = \tan\theta = \tan\varphi = \tan\theta' = 0$ to simplify the calculation. We also take the approximation:

$$
\kappa_2 \simeq 1, \qquad \kappa_3 \simeq s^2_W.
$$

In addition, W_5 and W'_4 make of a physical neutral non-Hermitian gauge boson X^0 which is defined by the combination:

$$
X^0_\mu \equiv \frac{W'_{4\mu} - iW_{5\mu}}{\sqrt{2}}. \tag{A.8}
$$

So we can rewrite the above covariance derivatives in the form below:

$$
\begin{aligned}
D_\mu^N &\simeq \partial_\mu + ieQA_\mu + ig_Z\big(T^3 - s_W^2 Q\big)Z_\mu + ig_{Z'}\big[\big(4c_W^2 - 1\big)\big(T^3 - Q\big) + 3c_W^2 X\big]Z'_\mu,\\
\bar{D}_\mu^N &\simeq \partial_\mu + ieQA_\mu + ig_Z\big(-T^3 - s_W^2 Q\big)Z_\mu + ig_{Z'}\big[\big(4c_W^2 - 1\big)\big(-T^3 - Q\big) + 3c_W^2 X\big]Z'_\mu,\\
D_{1\mu}^N &\simeq \partial_\mu + ieQA_\mu - ig_Z s_W^2 QZ_\mu + ig_{Z'}\big[-\big(4c_W^2 - 1\big)Q + 3c_W^2 X\big]Z'_\mu
\end{aligned}
\tag{A.9}
$$

where we have defined

$$
g_Z \equiv \frac{gc_\varphi}{c_W c_{\theta'}} \simeq \frac{g}{c_W} \quad \text{and} \quad g_{Z'} \equiv \frac{gc_\varphi \kappa_2}{c_W c_{\theta'} \kappa_1} \simeq \frac{g}{c_W \kappa_1}.
$$

For the charged gauginos, we have:

$$
\tilde{W}^\pm \equiv \frac{\lambda_V^1 \mp i\lambda_V^2}{\sqrt{2}}, \qquad \tilde{Y}^\pm \equiv \frac{\lambda_V^6 \pm i\lambda_V^7}{\sqrt{2}}. \tag{A.10}
$$

This leads to the covariant derivative of charged gauginos:

$$
\begin{aligned}
D_\mu^L \tilde{W}^\pm &\simeq \partial_\mu \tilde{W}^\pm \pm i(eA_\mu + gc_W Z_\mu)\tilde{W}^\pm = \partial_\mu \tilde{W}^\pm \pm i\big(eA_\mu + g_Z c_W^2 Z_\mu\big)\tilde{W}^\pm\\
&= \partial_\mu \tilde{W}^\pm + iQ_{\tilde{W}}\big(eA_\mu + g_Z c_W^2 Z_\mu\big)\tilde{W}^\pm,\\
D_\mu^L \tilde{Y}^\pm &= \partial_\mu \tilde{Y}^\pm \pm i\bigg(eA_\mu + g\frac{c_\varphi(c_{2W} + 2c_W^2 s_{\theta'}^2) + s_\varphi \kappa_1 \kappa_2}{2c_W c_{\theta'}} Z_\mu\\
&\quad + g\frac{s_\varphi(c_{2W} + 2c_W^2 s_{\theta'}^2) - c_\varphi \kappa_1 \kappa_2}{2c_W c_{\theta'}} Z'_\mu\bigg)\tilde{Y}^\pm\\
&\simeq \partial_\mu \tilde{Y}^\pm + iQ_{\tilde{Y}^\pm}\bigg(eA_\mu + \frac{1}{2}g_Z c_{2W} Z_\mu - \frac{1}{2}g_{Z'}\kappa_1^2 Z'_\mu\bigg)\tilde{Y}^\pm.
\end{aligned}
\tag{A.11}
$$

From these two formulas, we can deduce the vertices of neutral gauge boson–charged gaugino–charged gaugino.

A.3. Gauge boson–slepton–slepton interactions

This kind of vertex comes from the part [20]:

$$
\begin{aligned}
\mathcal{L}_{\tilde{l}\tilde{l}V} &= \frac{ig}{2}\big[\partial^\mu \bar{\tilde{L}}_i \lambda^a \tilde{L}_i - \bar{\tilde{L}}_i \lambda^a \partial^\mu \tilde{L}_i\big]V_\mu^a\\
&\quad + \frac{ig'}{\sqrt{6}}\bigg[-\frac{1}{3}\big(\partial^\mu \bar{\tilde{L}}_i \tilde{L}_i - \bar{\tilde{L}}_i \partial^\mu \tilde{L}_i\big) + \big(\partial^\mu \bar{\tilde{l}}^c \tilde{l}^c - \bar{\tilde{l}}^c \partial^\mu \tilde{l}^c\big)\bigg]B_\mu
\end{aligned}
$$

where $i = 1, 2, 3$ is the flavor index and $a = 1, 2, \ldots, 8$ is generator index of SU(3). For the $\{\tilde{\mu}, \tilde{\tau}\}$ sector with neutral boson we have:

$$
\begin{aligned}
\mathcal{L}_{\tilde{l}\tilde{l}V} &\simeq \frac{ig}{2}\bigg[\frac{1}{c_W}Z_\mu + \frac{c_{2W}}{\kappa_1 c_W}Z'_\mu\bigg] \times \big(\partial^\mu \bar{\tilde{\nu}}_\tau \tilde{\nu}_\tau - \bar{\tilde{\nu}}_\tau \partial^\mu \tilde{\nu}_\tau\big)\\
&\quad + \frac{ig}{2}\bigg[-2s_W A_\mu - \frac{c_{2W}}{c_W}Z_\mu + \frac{c_{2W}}{\kappa_1 c_W}Z'_\mu\bigg]\big(\partial^\mu \bar{\tilde{\tau}}\tilde{\tau} - \bar{\tilde{\tau}}\partial^\mu \tilde{\tau}\big)\\
&\quad + \frac{ig}{2}\bigg[-\frac{2c_W}{\kappa_1}Z'_\mu\bigg]\big(\partial^\mu \bar{\tilde{\nu}}_\tau^c \tilde{\nu}_\tau^c - \bar{\tilde{\nu}}_\tau^c \partial^\mu \tilde{\nu}_\tau^c\big) + (\tau \to \mu)
\end{aligned}
$$

Table 1
Photon vertices.

Vertex	Factor	Vertex	Factor
Photon–scalar–scalar (scalar φ: H, $\tilde{f}$)	$-ieQ_\varphi(p+p')^\mu$		
Photon–spinor–spinor (spinor ψ: fermion, Higgsino)	$-ieQ_\psi\bar{\sigma}^\mu$ $(ieQ_\psi\sigma^\mu)$	$\gamma\psi^c\psi^c$	$ieQ_\psi\bar{\sigma}^\mu$ $(-ieQ_\psi\sigma^\mu)$
Photon–boson–boson $W^{+\rho}W^{-\mu}A^\nu$	$ie[p_{+\rho}, p_{-\mu}, p_{A\nu}]$	$Y^{+\rho}Y^{-\mu}A^\nu$	$-ie[p_{+\rho}, p_{-\mu}, p_{A\nu}]$
Photon–Higgs–gauge boson $A^\mu W^\nu\rho_1$	$\frac{1}{2}(ieg)g_{\mu\nu}$	$A^\mu Y^\nu\rho_2$	$\frac{1}{2}(ieg)g_{\mu\nu}$
Photon–gaugino–gaugino $\overline{\tilde{W}^+}A_\mu\tilde{W}^+$	$-ie\bar{\sigma}^\mu$ (or $ie\sigma^\mu$)	$\overline{\tilde{W}^-}A_\mu\tilde{W}^-$	$ie\bar{\sigma}^\mu$ (or $-ie\sigma^\mu$)
$\overline{\tilde{Y}^+}A_\mu\tilde{Y}^+$	$-ie\bar{\sigma}^\mu$ (or $ie\sigma^\mu$)	$\overline{\tilde{Y}^-}A_\mu\tilde{Y}^-$	$ie\bar{\sigma}^\mu$ (or $-ie\sigma^\mu$)

$$
\begin{aligned}
&+\left[i\left(eA_\mu - etW Z_\mu + \frac{etW}{\kappa_1}Z'_\mu\right)\left(\partial^\mu\bar{\tilde{\tau}}^c\tilde{\tau}^c - \bar{\tilde{\tau}}^c\partial^\mu\tilde{\tau}^c\right) + \left(\tau^c\to\mu^c\right)\right]\\
&= i\left[\frac{1}{2}g_Z Z_\mu + \frac{1}{2}g_{Z'}c_{2W}Z'_\mu\right]\times\left(\partial^\mu\bar{\tilde{\nu}}_\tau\tilde{\nu}_\tau - \bar{\tilde{\nu}}_\tau\partial^\mu\tilde{\nu}_\tau\right)\\
&\quad - i\left[eA_\mu + \frac{1}{2}g_Z c_{2W}Z_\mu - \frac{1}{2}g_{Z'}c_{2W}Z'_\mu\right]\left(\partial^\mu\bar{\tilde{\tau}}\tilde{\tau} - \bar{\tilde{\tau}}\partial^\mu\tilde{\tau}\right)\\
&\quad - i\left[g_{Z'}c_W^2 Z'_\mu\right]\left(\partial^\mu\bar{\tilde{\nu}}^c_\tau\tilde{\nu}^c_\tau - \bar{\tilde{\nu}}^c_\tau\partial^\mu\tilde{\nu}^c_\tau\right) + (\tau\to\mu)\\
&\quad + \left[i\left(eA_\mu - g_Z s_W^2 Z_\mu + g_{Z'}s_W^2 Z'_\mu\right)\left(\partial^\mu\bar{\tilde{\tau}}^c\tilde{\tau}^c - \bar{\tilde{\tau}}^c\partial^\mu\tilde{\tau}^c\right)\right.\\
&\quad \left. + \left(\tau^c\to\mu^c\right)\right] \qquad \text{(A.12)}
\end{aligned}
$$

Interaction vertices of photon, Z and Z' bosons relating with our calculation are summarized in Tables 1, 2 and 3, respectively. We denote directions of momentums in Fig. 9. For simplicity, we omit spinor index in the formulas of boson–fermion–fermion vertices. The precise formulas of this kind of vertices is easily deduced using rules concerned in [12].

A.4. Mixing in the slepton sector

As we know, in supersymmetric models, in order to keep the conversation of LFV in the lepton sector at tree level, the sources of LFV are assumed to be from the slepton mass terms in the soft-breaking part of the Lagrangian [10,24]. For the SUSYE331, there are three mass terms of left-handed slepton, right-handed slepton and sneutrinos which may independently be sources of LFV. In addition, there exists another LFV source original from the Yukawa couplings between Higgs and neutrinos. Thus in the SUSYE331 model, there are at least four independent sources of LFV and we will parameterize them as follows. In each case of supersymmetric particle (sleptons) $\tilde{\psi}$ $(\psi = l_L, l_R, \nu_L, \nu_R)$, we define a corresponding mixing angle $\theta_{\tilde{\varphi}}$ which was defined in [21]. In what follows we just remind some general formulas for the review. The mass mixing matrices of smuon and stau as well as their sneutrinos can be written in the general form of:

Table 2
Z boson vertices.

Vertex	Factor	Vertex	Factor
$Z_\mu \tilde{\nu}_L^* \tilde{\nu}_L$	$-\frac{i}{2} g_Z (p+p')^\mu$		
$Z_\mu \tilde{\ell}_L^* \tilde{\ell}_L$	$\frac{i}{2} c_{2W} g_Z (p+p')^\mu$	$Z_\mu \tilde{\ell}_R^* \tilde{\ell}_R$	$i g_Z s_W^2 (p+p')^\mu$
$\rho^{0*} \rho^0 Z_\mu$	$\frac{i}{2} g_Z (p+p')^\mu$	$\rho'^{0*} \rho'^0 Z_\mu$	$-\frac{i}{2} g_Z (p+p')^\mu$
$\chi_1^{0*} \chi_1^0 Z_\mu$	$-\frac{i}{2} g_Z (p+p')^\mu$	$\chi_1'^{0*} \chi_1'^0 Z_\mu$	$\frac{i}{2} g_Z (p+p')^\mu$
$\overline{\tilde{\rho}^0} \tilde{\rho}^0 Z_\mu$	$\frac{i}{2} g_Z \bar{\sigma}^\mu$ (or $-\frac{i}{2} g_Z \sigma^\mu$)	$\overline{\tilde{\rho}'^0} \tilde{\rho}'^0 Z_\mu$	$-\frac{i}{2} g_Z \sigma^\mu$ (or $\frac{i}{2} g_Z \sigma^\mu$)
$\overline{\tilde{\rho}_1^+} \tilde{\rho}_1^+ Z_\mu$	$-\frac{i}{2} g_Z c_{2W} \bar{\sigma}^\mu$ (or $\frac{i}{2} g_Z c_{2W} \sigma^\mu$)	$\overline{\tilde{\rho}_1'^-} \tilde{\rho}_1'^- Z_\mu$	$\frac{i}{2} g_Z c_{2W} \sigma^\mu$ (or $-\frac{i}{2} g_Z c_{2W} \sigma^\mu$)
$\overline{\tilde{\rho}_2^+} \tilde{\rho}_2^+ Z_\mu$	$\frac{i}{2} g_Z s_W^2 \bar{\sigma}^\mu$ (or $-\frac{i}{2} g_Z s_W^2 \sigma^\mu$)	$\overline{\tilde{\rho}_2'^-} \tilde{\rho}_2'^- Z_\mu$	$-\frac{i}{2} g_Z s_W^2 \sigma^\mu$ (or $\frac{i}{2} g_Z s_W^2 \sigma^\mu$)
$\overline{\tilde{W}^+} Z_\mu \tilde{W}^+$	$-i g_Z c_W^2 \bar{\sigma}^\mu$ (or $i g_Z c_W^2 \sigma^\mu$)	$\overline{\tilde{W}^-} Z_\mu \tilde{W}^-$	$i g_Z c_W^2 \bar{\sigma}^\mu$ (or $-i g_Z c_W^2 \sigma^\mu$)
$\overline{\tilde{Y}^+} Z_\mu \tilde{Y}^+$	$-\frac{i}{2} g_Z c_{2W} \bar{\sigma}^\mu$ (or $\frac{i}{2} g_Z c_{2W} \sigma^\mu$)	$\overline{\tilde{Y}^-} Z_\mu \tilde{Y}^-$	$\frac{i}{2} g_Z c_{2W} \bar{\sigma}^\mu$ (or $-\frac{i}{2} g_Z c_{2W} \sigma^\mu$)

Table 3
Z' boson vertices.

Vertex	Factor	Vertex	Factor
$Z'_\mu \tilde{\nu}_L^* \tilde{\nu}_L$	$-\frac{i}{2} g_{Z'} c_{2W} (p+p')^\mu$	$Z'_\mu \tilde{\nu}_R^* \tilde{\nu}_R$	$-g_{Z'} c_W^2 (p+p')^\mu$
$Z'_\mu \tilde{\ell}_L^* \tilde{\ell}_L$	$-\frac{i}{2} c_{2W} g_{Z'} (p+p')^\mu$	$Z'_\mu \tilde{\ell}_R^* \tilde{\ell}_R$	$-i g_{Z'} s_W^2 (p+p')^\mu$
$\rho^{0*} \rho^0 Z'_\mu$	$-\frac{i}{2} g_Z (p+p')^\mu$	$\rho'^{0*} \rho'^0 Z'_\mu$	$\frac{i}{2} g_Z (p+p')^\mu$
$\chi_1^{0*} \chi_1^0 Z'_\mu$	$-\frac{i}{2} g_{Z'} c_{2W} (p+p')^\mu$	$\chi_1'^{0*} \chi_1'^0 Z'_\mu$	$\frac{i}{2} g_{Z'} c_{2W} (p+p')^\mu$
$\chi_2^{0*} \chi_2^0 Z'_\mu$	$-\frac{i}{2} g_{Z'} c_W^2 (p+p')^\mu$	$\chi_2'^{0*} \chi_2'^0 Z'_\mu$	$\frac{i}{2} g_{Z'} c_W^2 (p+p')^\mu$
$\overline{\tilde{\rho}^0} \tilde{\rho}^0 Z'_\mu$	$-\frac{i}{2} g_{Z'} \bar{\sigma}^\mu$ (or $\frac{i}{2} g_{Z'} \sigma^\mu$)	$\overline{\tilde{\rho}'^0} \tilde{\rho}'^0 Z_\mu$	$\frac{i}{2} g_{Z'} \sigma^\mu$ (or $-\frac{i}{2} g_{Z'} \sigma^\mu$)
$\overline{\tilde{\rho}_1^+} \tilde{\rho}_1^+ Z'_\mu$	$-\frac{i}{2} g_{Z'} \bar{\sigma}^\mu$ (or $\frac{i}{2} g_{Z'} \sigma^\mu$)	$\overline{\tilde{\rho}_1'^-} \tilde{\rho}_1'^- Z'_\mu$	$\frac{i}{2} g_{Z'} \sigma^\mu$ (or $-\frac{i}{2} g_{Z'} \sigma^\mu$)
$\overline{\tilde{\rho}_2^+} \tilde{\rho}_2^+ Z'_\mu$	$\frac{i}{2} g_{Z'} \bar{\sigma}^\mu$ (or $-\frac{i}{2} g_{Z'} \sigma^\mu$)	$\overline{\tilde{\rho}_2'^-} \tilde{\rho}_2'^- Z'_\mu$	$-\frac{i}{2} g_{Z'} c_{2W} \sigma^\mu$ (or $\frac{i}{2} g_Z c_{2W} \sigma^\mu$)
$\overline{\tilde{Y}^+} Z'_\mu \tilde{Y}^+$	$\frac{i}{2} g_{Z'} \kappa_1^2 \bar{\sigma}^\mu$ (or $-\frac{i}{2} g_{Z'} \kappa_1^2 \sigma^\mu$)	$\overline{\tilde{Y}^-} Z'_\mu \tilde{Y}^-$	$-\frac{i}{2} g_{Z'} \kappa_1^2 \bar{\sigma}^\mu$ (or $\frac{i}{2} g_{Z'} \kappa_1^2 \sigma^\mu$)

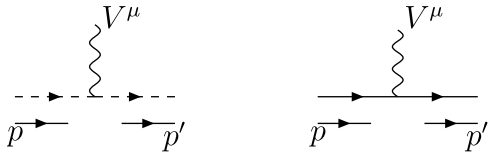

Fig. 9. Notations of directions of scalars and fermions. Here V^μ denotes a photon A, Z or Z' boson.

$$\mathcal{M}^2_{\tilde{\psi}} = \begin{pmatrix} m^2_{\tilde{\psi}_{\mu\mu}} & m^2_{\tilde{\psi}_{\mu\tau}} \\ m^2_{\tilde{\psi}_{\mu\tau}} & m^2_{\tilde{\psi}_{\tau\tau}} \end{pmatrix}. \tag{A.13}$$

Mixing angles then can be determined as

$$s_{\tilde{\psi}} \equiv \sin\theta_{\tilde{\psi}}, \qquad c_{\tilde{\psi}} \equiv \cos\theta_{\tilde{\psi}} \quad \text{where } s_{\tilde{\psi}} c_{\tilde{\psi}} = \frac{m^2_{\tilde{\psi}_{\mu\tau}}}{m^2_{\psi_2} - m^2_{\psi_3}}, \tag{A.14}$$

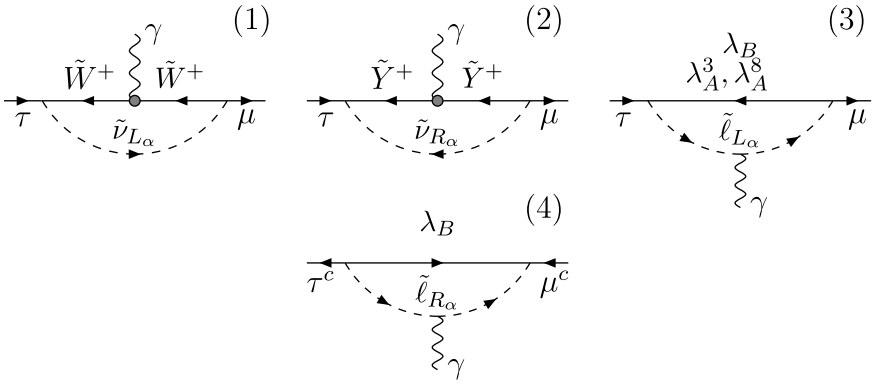

Fig. 10. Diagrams contributing to $C^{\gamma}_{L,R}$.

where $s_{\tilde{\psi}} = \{s_L, s_R, s_{\tilde{\nu}_L}, s_{\tilde{\nu}_R}\}$ and $\{m^2_{\tilde{\psi}_2}, m^2_{\tilde{\psi}_3}\}$ are eigenvalues of $\mathcal{M}^2_{\tilde{\psi}}$, according to notations in [21]. In addition, for convenience we denote $m^2_{\tilde{\psi}}$ instead of $\tilde{m}^2_{\psi}$. We always choose $m^2_{\tilde{\psi}_3} < m^2_{\tilde{\psi}_2}$ to take the positive values of $s_{\tilde{\psi}}$ and $c_{\tilde{\psi}}$. The mass-eigenstates of sleptons are denoted as $\{\tilde{\psi}_2, \tilde{\psi}_3\}$ while the flavor-eigenstates are $\{\tilde{\psi}_\mu, \tilde{\psi}_\tau\}$. The relation between two bases are:

$$\tilde{\psi}_\mu = c_{\tilde{\psi}}\tilde{\psi}_2 - s_{\tilde{\psi}}\tilde{\psi}_3 \quad \text{and} \quad \tilde{\psi}_\tau = s_{\tilde{\psi}}\tilde{\psi}_2 + c_{\tilde{\psi}}\tilde{\psi}_3. \tag{A.15}$$

Appendix B. Contribution to $\tau \to \mu\gamma$

Diagrams relating to $C^{\gamma}_{L,R}$ are drawn in Fig. 10 with no line of Higgs insertion. Formulas of $C^{\gamma}_{L,R}$ are:

$$\begin{aligned}
C^{\gamma}_L &= \frac{(g^2 c_L s_L)}{16\pi^2} \times \frac{1}{9}\big[-K_5\big(m^2_\lambda, m^2_{\tilde{l}_{L2}}, m^2_{\tilde{l}_{L2}}, m^2_{\tilde{l}_{L2}}, m^2_{\tilde{l}_{L2}}\big)\big] \\
&\quad + \frac{(g^2 c_{\nu_L} s_{\nu_L})}{16\pi^2} \times \frac{1}{6}\big[-2K_5\big(m^2_\lambda, m^2_\lambda, m^2_\lambda, m^2_\lambda, \tilde{m}^2_{\nu_{L2}}\big) \\
&\quad + 3m^2_\lambda J_5\big(m^2_\lambda, m^2_\lambda, m^2_\lambda, m^2_\lambda, \tilde{m}^2_{\nu_{L2}}\big)\big] \\
&\quad + \frac{(g^2 c_{\nu_R} s_{\nu_R})}{16\pi^2} \times \frac{1}{6}\big[-2K_5\big(m^2_\lambda, m^2_\lambda, m^2_\lambda, m^2_\lambda, \tilde{m}^2_{\nu_{R2}}\big) \\
&\quad + 3m^2_\lambda J_5\big(m^2_\lambda, m^2_\lambda, m^2_\lambda, m^2_\lambda, \tilde{m}^2_{\nu_{R2}}\big)\big] \\
&\quad + \frac{g'^2 c_L s_L}{16\pi^2} \times \frac{1}{162}\big[-K_5\big(m^2_B, m^2_{\tilde{l}_{L2}}, m^2_{\tilde{l}_{L2}}, m^2_{\tilde{l}_{L2}}, m^2_{\tilde{l}_{L2}}\big)\big] \\
&\quad - (L_2 \to L_3, R_2 \to R_3), \\
C^{\gamma}_R &= \frac{g'^2 c_R s_R}{16\pi^2} \times \frac{1}{18}\big[-K_5\big(m^2_B, m^2_{\tilde{l}_{R2}}, m^2_{\tilde{l}_{R2}}, m^2_{\tilde{l}_{R2}}, m^2_{\tilde{l}_{R2}}\big)\big] - [R_2 \to R_3].
\end{aligned} \tag{B.1}$$

On the other hand, D^{γ} gets contributions from diagrams with one line Higgs insertion, Figs. 11,12 and 13. There is another class of LFV sources relating with neutrino-mediation in which their contributions are very small [22] so we will ignore them in our investigation. The $D^{\gamma}_{L,R}$ can be separated into three parts:

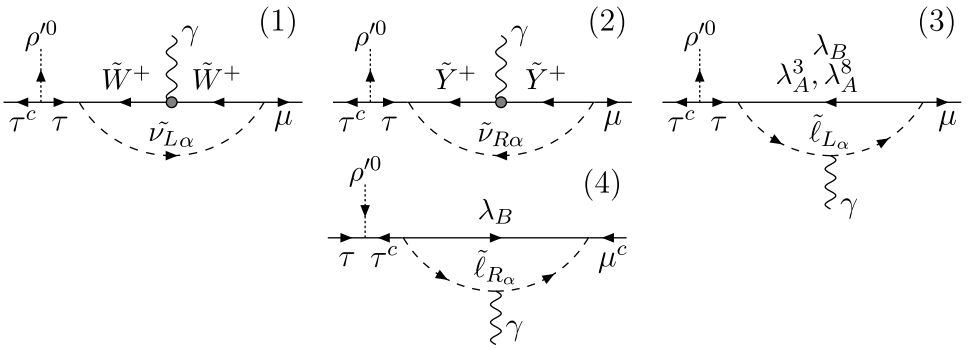

Fig. 11. Contribution to $D_L^{\gamma(a)}$ [1–3] and $D_R^{\gamma(a)}$ [4].

$$D_{L,R}^{\gamma} = D_{L,R}^{\gamma(a)} + D_{L,R}^{\gamma(b)} + D_{L,R}^{\gamma(c)},$$

where diagrams involving each part are expressed in Figs. 11, 12 and 13.

For $D^{\gamma(a)}$:

$$\begin{aligned}
D_L^{\gamma(a)} &= \frac{g^2 c_L s_L}{16\pi^2} \times \frac{1}{3}\big[m_{\tilde{l}_{L2}}^2 J_5\big(m_\lambda^2, m_{\tilde{l}_{L2}}^2, m_{\tilde{l}_{L2}}^2, m_{\tilde{l}_{L2}}^2, m_{\tilde{l}_{L2}}^2\big)\big] \\
&\quad - \frac{g^2 c_{\nu_L} s_{\nu_L}}{16\pi^2} \times \frac{1}{2}\big[m_\lambda^2 J_5\big(m_\lambda^2, m_\lambda^2, m_\lambda^2, m_\lambda^2, m_{\tilde{\nu}_{L2}}^2\big)\big] \\
&\quad - \frac{g^2 c_{\nu_R} s_{\nu_R}}{16\pi^2} \times \frac{1}{2}\big[m_\lambda^2 J_5\big(m_\lambda^2, m_\lambda^2, m_\lambda^2, m_\lambda^2, m_{\tilde{\nu}_{R2}}^2\big)\big] \\
&\quad + \frac{g'^2 c_L s_L}{16\pi^2} m_{\tilde{l}_{L2}}^2 \left[\frac{1}{54} J_5\big(m_B^2, m_{\tilde{l}_{L2}}^2, m_{\tilde{l}_{L2}}^2, m_{\tilde{l}_{L2}}^2, m_{\tilde{l}_{L2}}^2\big)\right] \\
&\quad - [L_2 \to L_3, R_2 \to R_3], \\
D_R^{\gamma(a)} &= \frac{g'^2 c_R s_R}{16\pi^2} m_{\tilde{l}_{R2}}^2 \left[\frac{1}{6} J_5\big(m_B^2, m_{\tilde{l}_{R2}}^2, m_{\tilde{l}_{R2}}^2, m_{\tilde{l}_{R2}}^2, m_{\tilde{l}_{R2}}^2\big)\right] - [R_2 \to R_3].
\end{aligned} \tag{B.2}$$

For $D^{\gamma(b)}$:

$$\begin{aligned}
D_L^{\gamma(b)} &= -\frac{g^2 s_{\nu_L} c_{\nu_L}}{16\pi^2} m_{\tilde{\nu}_{L2}}^4 I_5\big(m_\lambda^2, \mu_\rho^2, m_{\tilde{\nu}_{L2}}^2, m_{\tilde{\nu}_{L2}}^2, m_{\tilde{\nu}_{L2}}^2\big) \\
&\quad - \frac{g^2 s_{\nu_R} c_{\nu_R}}{16\pi^2} m_{\tilde{\nu}_{R2}}^4 I_5\big(m_\lambda^2, \mu_\rho^2, m_{\tilde{\nu}_{R2}}^2, m_{\tilde{\nu}_{R2}}^2, m_{\tilde{\nu}_{R2}}^2\big) \\
&\quad + \frac{g^2 s_{\nu_{L2}} c_{\nu_{L2}}}{16\pi^2} \times m_\lambda \mu \tan\gamma \big[J_5\big(m_\lambda^2, m_\lambda^2, \mu_\rho^2, \mu_\rho^2, m_{\tilde{\nu}_{L2}}^2\big) \\
&\quad + J_5\big(m_\lambda^2, m_\lambda^2, m_\lambda^2, \mu_\rho^2, m_{\tilde{\nu}_{L2}}^2\big) + J_5\big(m_\lambda^2, \mu_\rho^2, \mu_\rho^2, \mu_\rho^2, m_{\tilde{\nu}_{L2}}^2\big)\big] \\
&\quad + \frac{g^2 s_{\nu_{R2}} c_{\nu_{R2}}}{16\pi^2} \times m_\lambda \mu \tan\gamma \big[J_5\big(m_\lambda^2, m_\lambda^2, \mu_\rho^2, \mu_\rho^2, m_{\tilde{\nu}_{R2}}^2\big) \\
&\quad + J_5\big(m_\lambda^2, m_\lambda^2, m_\lambda^2, \mu_\rho^2, m_{\tilde{\nu}_{L2}}^2\big) + J_5\big(m_\lambda^2, \mu_\rho^2, \mu_\rho^2, \mu_\rho^2, m_{\tilde{\nu}_{R2}}^2\big)\big] \\
&\quad - \frac{g^2 s_L c_L}{16\pi^2} m_{\tilde{l}_{L2}}^2 \times \frac{2}{3}\big[J_5\big(m_\lambda^2, \mu_\rho^2, m_{\tilde{l}_{L2}}^2, m_{\tilde{l}_{L2}}^2, m_{\tilde{l}_{L2}}^2\big) \\
&\quad - m_\lambda \mu_\rho \tan\gamma\ I_5\big(m_\lambda^2, \mu_\rho^2, m_{\tilde{l}_{L2}}^2, m_{\tilde{l}_{L2}}^2, m_{\tilde{l}_{L2}}^2\big)\big]
\end{aligned}$$

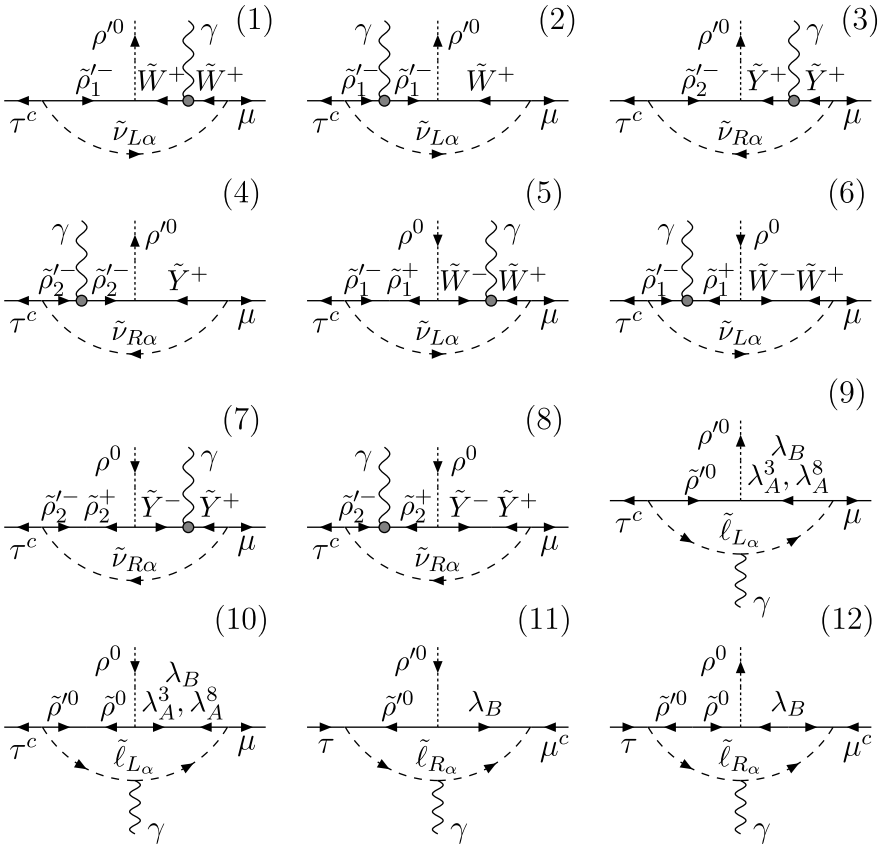

Fig. 12. Contribution to $D_L^{\gamma(b)}$ [1–10] and $D_R^{\gamma(b)}$ [11, 12].

$$
\begin{aligned}
&+\frac{g'^2 s_L c_L}{16\pi^2} m^2_{\tilde{l}_{L2}} \times \frac{2}{27}\big[J_5\big(m_B^2,\mu_\rho^2,m^2_{\tilde{l}_{L2}},m^2_{\tilde{l}_{L2}},m^2_{\tilde{l}_{L2}}\big)\\
&-m_B\mu\tan\gamma\, I_5\big(m_B^2,\mu_\rho^2,m^2_{\tilde{l}_{L2}},m^2_{\tilde{l}_{L2}},m^2_{\tilde{l}_{L2}}\big)\big]-[L_2\to L_3],\\
D_R^{\gamma(b)} &= \frac{g'^2 s_R c_R}{16\pi^2} m^2_{\tilde{l}_{R2}} \times \frac{2}{9}\big[-J_5\big(m_B^2,\mu_\rho^2,m^2_{\tilde{l}_{R2}},m^2_{\tilde{l}_{R2}},m^2_{\tilde{l}_{R2}}\big)\\
&+m_B\mu_\rho\tan\gamma\, I_5\big(m_B^2,\mu_\rho^2,m^2_{\tilde{l}_{R2}},m^2_{\tilde{l}_{R2}},m^2_{\tilde{l}_{R2}}\big)\big]-[R_2\to R_3]. \qquad \text{(B.3)}
\end{aligned}
$$

For $D^{\gamma(c)}$:

$$
\begin{aligned}
D_L^{\gamma(c)} = &-\frac{g'}{16\pi^2}\,\frac{m_B^3}{9}\times\Bigg\{\Bigg[s_L c_L\Bigg(s_R^2\Bigg[A_\tau+\frac{1}{2}\mu_\rho\tan\gamma\Bigg]+s_R c_R A^R_{\mu\tau}\Bigg)+c_L^2 s_R^2 A^L_{\mu\tau}\Bigg]\\
&\times I_5\big(m_B^2,m_B^2,m_B^2,m^2_{\tilde{l}_{L2}},m^2_{\tilde{l}_{R2}}\big)\\
&-\Bigg[s_L c_L\Bigg(s_R^2\Bigg[A_\tau+\frac{1}{2}\mu_\rho\tan\gamma\Bigg]+s_R c_R A^R_{\mu\tau}\Bigg)-s_L^2 s_R^2 A^L_{\mu\tau}\Bigg]\\
&\times I_5\big(m_B^2,m_B^2,m_B^2,m^2_{\tilde{l}_{L3}},m^2_{\tilde{l}_{R2}}\big)
\end{aligned}
$$

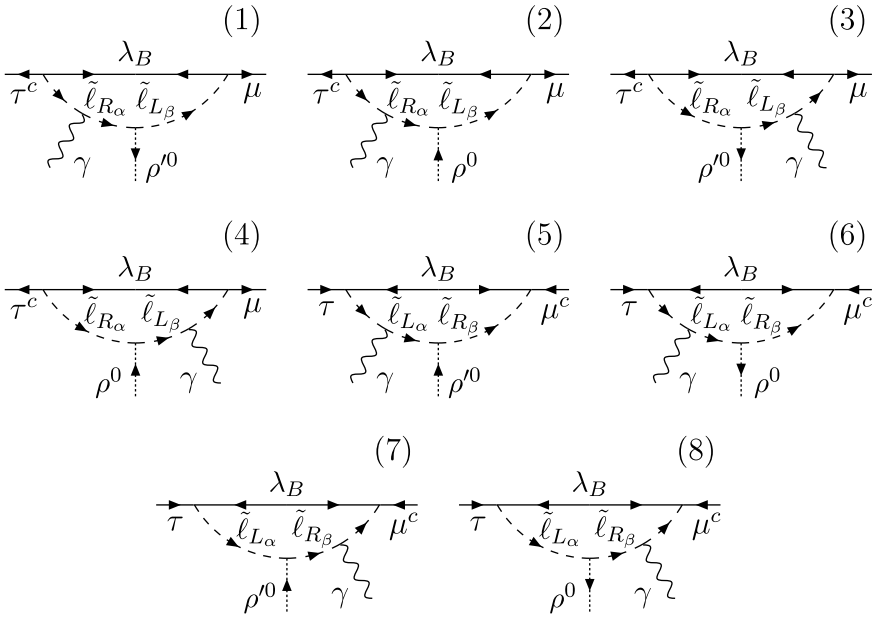

Fig. 13. Contribution to $D_L^{\gamma(c)}$ [1–6] and D_R^{γ} [7, 8].

$$
\begin{aligned}
&+\left[s_L c_L\left(c_R^2\left[A_\tau+\frac{1}{2}\mu_\rho\tan\gamma\right]-s_R c_R A_{\mu\tau}^R\right)+c_L^2 c_R^2 A_{\mu\tau}^L\right]\\
&\times I_5\big(m_B^2,m_B^2,m_B^2,m_{\tilde{l}_{L2}}^2,m_{\tilde{l}_{R3}}^2\big)\\
&-\left[s_L c_L\left(c_R^2\left[A_\tau+\frac{1}{2}\mu_\rho\tan\gamma\right]-s_R c_R A_{\mu\tau}^R\right)-s_L^2 c_R^2 A_{\mu\tau}^L\right]\\
&\times I_5\big(m_B^2,m_B^2,m_B^2,m_{\tilde{l}_{L3}}^2,m_{\tilde{l}_{R3}}^2\big)\Bigg\},\\
D_R^{\gamma(c)}=&-\frac{g'}{16\pi^2}\frac{m_B^3}{9}\times\Bigg\{\left[s_R c_R\left(s_L^2\left[A_\tau+\frac{1}{2}\mu_\rho\tan\gamma\right]+s_L c_L A_{\mu\tau}^L\right)+c_R^2 s_L^2 A_{\mu\tau}^R\right]\\
&\times I_5\big(m_B^2,m_B^2,m_B^2,m_{\tilde{l}_{L2}}^2,m_{\tilde{l}_{R2}}^2\big)\\
&-\left[s_R c_R\left(s_L^2\left[A_\tau+\frac{1}{2}\mu_\rho\tan\gamma\right]+s_L c_L A_{\mu\tau}^L\right)-s_R^2 s_L^2 A_{\mu\tau}^R\right]\\
&\times I_5\big(m_B^2,m_B^2,m_B^2,m_{\tilde{l}_{L2}}^2,m_{\tilde{l}_{R3}}^2\big)\\
&+\left[s_R c_R\left(c_L^2\left[A_\tau+\frac{1}{2}\mu_\rho\tan\gamma\right]-s_L c_L A_{\mu\tau}^L\right)+c_R^2 c_L^2 A_{\mu\tau}^R\right]\\
&\times I_5\big(m_B^2,m_B^2,m_B^2,m_{\tilde{l}_{L3}}^2,m_{\tilde{l}_{R2}}^2\big)\\
&-\left[s_R c_R\left(c_L^2\left[A_\tau+\frac{1}{2}\mu_\rho\tan\gamma\right]-s_L c_L A_{\mu\tau}^L\right)-s_R^2 c_L^2 A_{\mu\tau}^R\right]\\
&\times I_5\big(m_B^2,m_B^2,m_B^2,m_{\tilde{l}_{L3}}^2,m_{\tilde{l}_{R3}}^2\big)\Bigg\}.
\end{aligned}
\tag{B.4}
$$

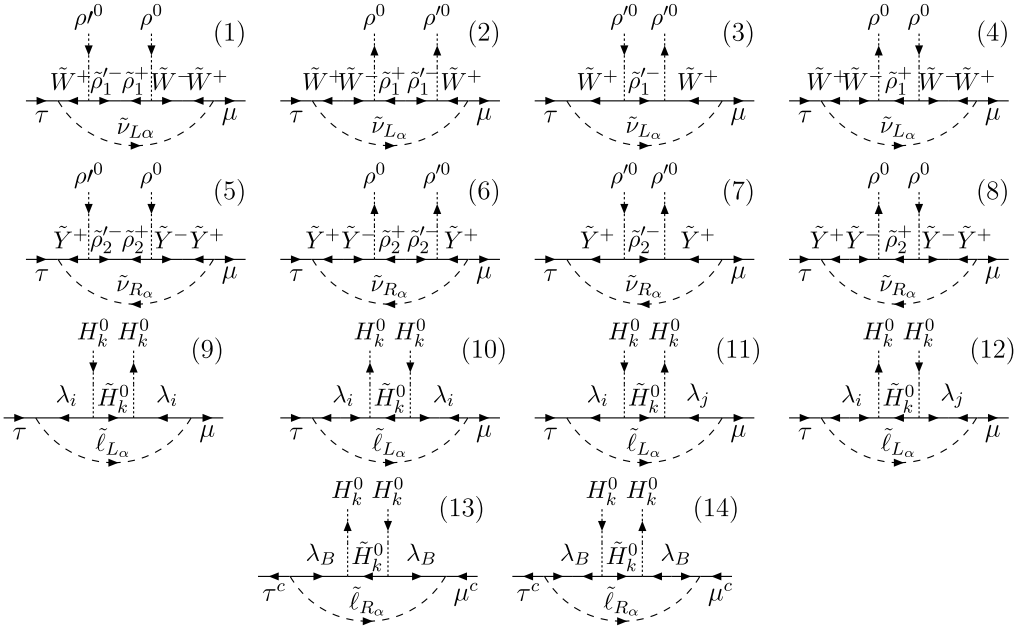

Fig. 14. Diagrams contributing to $A_L^{Z(a)}$ (or $A_L^{1Z'(a)}$) (first, second and third rows) and $A_R^{Z(a)}$ (or $A_R^{1Z'(a)}$) (fourth row). Here we denote $H_k^0 \in \{\rho^0, \rho'^0\}$ while $\lambda_{i,j}$ implies $i, j = \{B, 3, 8\}$ and $i \neq j$.

Appendix C. Contributions to $Z \to \mu\tau$

In this appendix, we draw all the possible diagrams which contribute to the effective operator $Z \to \mu\tau$ in the limit of assumption given out in [10]. All of these diagrams can be applied to the case of Z' boson.

C.1. Contributions to $A_{L,R}^Z$

Diagrams contributing to $A_{L,R}^{Z(a)}$ are shown in Fig. 14. The formulas are:

$$
\begin{aligned}
A_L^{Z(a)} &= (s_{\nu_L} c_{\nu_L}) \times \frac{g^2 c_W^2}{16\pi^2} \times \frac{1}{4}(1 + c_{2\gamma}) \\
&\quad \times \left[-\mu_\rho^2 J_5\left(m_\lambda^2, m_\lambda^2, \mu_\rho^2, \mu_\rho^2, m_{\tilde{\nu}_{L2}}^2\right) - 2J_4\left(m_\lambda^2, m_\lambda^2, \mu_\rho^2, m_{\tilde{\nu}_{L2}}^2\right)\right] \\
&\quad + (s_{\nu_R} c_{\nu_R}) \times \frac{g^2 c_W^2}{16\pi^2} \times \frac{1}{4}(1 + c_{2\gamma}) \\
&\quad \times \left[-\mu_\rho^2 J_5\left(m_\lambda^2, m_\lambda^2, \mu_\rho^2, \mu_\rho^2, m_{\tilde{\nu}_{R2}}^2\right) - 2J_4\left(m_\lambda^2, m_\lambda^2, \mu_\rho^2, m_{\tilde{\nu}_{R2}}^2\right)\right] \\
&\quad + (s_L c_L) \times \frac{g^2 c_W^2}{16\pi^2} \times \frac{11}{36} c_{2\gamma} \\
&\quad \times \left[-\mu_\rho^2 J_5\left(m_\lambda^2, m_\lambda^2, \mu_\rho^2, \mu_\rho^2, m_{\tilde{l}_{L2}}^2\right) - 2J_4\left(m_\lambda^2, m_\lambda^2, \mu_\rho^2, m_{\tilde{l}_{L2}}^2\right)\right. \\
&\quad \left. + m_\lambda^2\left(I_4\left(m_\lambda^2, m_\lambda^2, \mu_\rho^2, m_{\tilde{l}_{L2}}^2\right) - \mu_\rho^2 I_5\left(m_\lambda^2, m_\lambda^2, \mu_\rho^2, \mu_\rho^2, m_{\tilde{l}_{L2}}^2\right)\right)\right]
\end{aligned}
$$

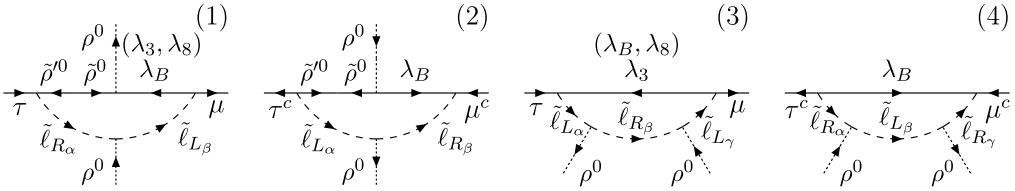

Fig. 15. Diagrams contributing to $A_{L,R}^{Z(b)}$ (left side) and $A_{L,R}^{Z(c)}$ (right side) in SUSYE331.

$$
\begin{aligned}
&- (s_{\nu_L} c_{\nu_L}) \times \frac{g^2 c_W^2 m_\lambda^2}{16\pi^2} \times \frac{1}{4}(1 - c_{2\gamma}) \\
&\times \left[\mu_\rho^2 I_5\left(m_\lambda^2, m_\lambda^2, \mu_\rho^2, \mu_\rho^2, m_{\tilde{\nu}_{L2}}^2\right) - I_4\left(m_\lambda^2, m_\lambda^2, \mu_\rho^2, m_{\tilde{\nu}_{L2}}^2\right)\right] \\
&- (s_{\nu_R} c_{\nu_R}) \times \frac{g^2 c_W^2 m_\lambda^2}{16\pi^2} \times \frac{1}{4}(1 - c_{2\gamma}) \\
&\times \left[\mu_\rho^2 I_5\left(m_\lambda^2, m_\lambda^2, \mu_\rho^2, \mu_\rho^2, m_{\tilde{\nu}_{R2}}^2\right) - I_4\left(m_\lambda^2, m_\lambda^2, \mu_\rho^2, m_{\tilde{\nu}_{R2}}^2\right)\right] \\
&+ (s_L c_L) \times \frac{g'^2 c_W^2}{16\pi^2} \times \frac{8}{81} c_{2\gamma} \\
&\times \left\{\mu_\rho^2 J_5\left(m_B^2, m_\lambda^2, \mu_\rho^2, \mu_\rho^2, m_{\tilde{l}_{L2}}^2\right) + 2J_4\left(m_B^2, m_\lambda^2, \mu_\rho^2, m_{\tilde{l}_{L2}}^2\right)\right. \\
&\left. - m_B m_\lambda\left[\mu_\rho^2 I_5\left(m_B^2, m_\lambda^2, \mu_\rho^2, \mu_\rho^2, m_{\tilde{l}_{L2}}^2\right) - I_4\left(m_B^2, m_\lambda^2, \mu_\rho^2, m_{\tilde{l}_{L2}}\right)\right]\right\} \\
&+ (s_{\nu_L} c_{\nu_L}) \times \frac{g^2 c_W^2}{16\pi^2} \times \frac{1}{2} s_{2\gamma}\left[\mu_\rho m_\lambda J_5\left(m_\lambda^2, m_\lambda^2, \mu_\rho^2, \mu_\rho^2, m_{\tilde{\nu}_{L2}}^2\right)\right] \\
&+ (s_{\nu_R} c_{\nu_R}) \times \frac{g^2 c_W^2}{16\pi^2} \times \frac{1}{2} s_{2\gamma}\left[\mu_\rho m_\lambda J_5\left(m_\lambda^2, m_\lambda^2, \mu_\rho^2, \mu_\rho^2, m_{\tilde{\nu}_{R2}}^2\right)\right] \\
&+ (s_L c_L) \times \frac{g'^2 t^2 c_W^2}{16\pi^2} \times \frac{2}{729} c_{2\gamma} \\
&\times \left[-\mu_\rho^2 J_5\left(m_B^2, m_B^2, \mu_\rho^2, \mu_\rho^2, m_{\tilde{l}_{L2}}^2\right) - 2J_4\left(m_B^2, m_B^2, \mu_\rho^2, m_{\tilde{l}_{L2}}^2\right)\right. \\
&\left. + m_B^2\left(\mu_\rho^2 I_5\left(m_B^2, m_B^2, \mu_\rho^2, \mu_\rho^2, m_{\tilde{l}_{L2}}^2\right) - I_4\left(m_B^2, m_B^2, \mu_\rho^2, m_{\tilde{l}_{L2}}^2\right)\right)\right] \\
&- (L_2 \to L_3, R_2 \to R_3), \qquad \text{(C.1)}
\end{aligned}
$$

$$
\begin{aligned}
A_R^{Z(a)} &= (s_R c_R) \frac{g'^2 t^2 c_W^2}{16\pi^2} \times \frac{2}{81} c_{2\gamma} \\
&\times \left\{\mu_\rho^2 J_5\left(m_B^2, m_B^2, \mu_\rho^2, \mu_\rho^2, m_{\tilde{l}_{R2}}^2\right) + 2J_4\left(m_B^2, m_B^2, \mu_\rho^2, m_{\tilde{l}_{R2}}^2\right)\right. \\
&- m_B^2\left[\mu_\rho^2 I_5\left(m_B^2, m_B^2, \mu_\rho^2, \mu_\rho^2, m_{\tilde{l}_{R2}}^2\right)\right. \\
&\left.\left. - I_4\left(m_B^2, m_B^2, \mu_\rho^2, m_{\tilde{l}_{R2}}^2\right)\right]\right\} - [R_2 \to R_3]. \qquad \text{(C.2)}
\end{aligned}
$$

For $A_{L,R}^{Z(b,c)}$, see Fig. 15.

Formula for $A_L^{Z(b)}$:

$$
\begin{aligned}
A_L^{Z(b)} &= (s_L c_L) \times \frac{m_\tau^2 c_W^2}{16\pi^2 V^2} \times \frac{1}{3}\left(t_\gamma^2 \mu_\rho^2\right)\left[s_R^2\left(J_5\left(m_\lambda^2, \mu_\rho^2, \mu_\rho^2, m_{\tilde{l}_{L_2}}^2, m_{\tilde{l}_{R_2}}^2\right)\right.\right. \\
&\left.\left. + J_5\left(m_\lambda^2, \mu_\rho^2, m_{\tilde{l}_{L_2}}^2, m_{\tilde{l}_{R_2}}^2, m_{\tilde{l}_{R_2}}^2\right)\right) + c_R^2\left(J_5\left(m_\lambda^2, \mu_\rho^2, \mu_\rho^2, m_{\tilde{l}_{L_2}}^2, m_{\tilde{l}_{R_3}}^2\right)\right.\right.
\end{aligned}
$$

$$
\begin{aligned}
&+ J_5\big(m_\lambda^2, \mu_\rho^2, m_{\tilde{l}_{L_2}}^2, m_{\tilde{l}_{R_3}}^2, m_{\tilde{l}_{R_3}}^2\big)\big)\big] \\
&+ (s_L c_L) \times \frac{m_\tau^2 t^2 c_W^2}{16\pi^2\, V^2} \times \frac{1}{27}\big(t_\gamma^2 \mu_\rho^2\big)\big[-s_R^2\big(J_5\big(m_B^2, \mu_\rho^2, \mu_\rho^2, m_{\tilde{l}_{L2}}^2, m_{\tilde{l}_{R2}}^2\big) \\
&+ J_5\big(m_B^2, \mu_\rho^2, m_{\tilde{l}_{L2}}^2, m_{\tilde{l}_{R2}}^2, m_{\tilde{l}_{R2}}^2\big)\big) - c_R^2\big(J_5\big(m_B^2, \mu_\rho^2, \mu_\rho^2, m_{\tilde{l}_{L2}}^2, m_{\tilde{l}_{R3}}^2\big) \\
&+ J_5\big(m_B^2, \mu_\rho^2, m_{\tilde{l}_{L2}}^2, m_{\tilde{l}_{R3}}^2, m_{\tilde{l}_{R3}}^2\big)\big)\big] - (L_2 \to L_3),
\end{aligned} \tag{C.3}
$$

where $m_\tau = Y_\tau \times v'/\sqrt{2}$ is mass of the tau and $V \equiv v_{\text{weak}} = \sqrt{v^2 + v'^2}$ in the SUSYE331 model. We also have formula of $A_R^{Z(b)}$:

$$
\begin{aligned}
A_R^{Z(b)} &= (s_R c_R) \times \frac{m_\tau^2 t^2 c_W^2}{16\pi^2\, V^2} \times \frac{1}{9} t_\gamma^2 \mu_\rho^2\big[-s_L^2\big(J_5\big(m_B^2, \mu_\rho^2, \mu_\rho^2, m_{\tilde{l}_{L_2}}^2, m_{\tilde{l}_{R_2}}^2\big) \\
&+ J_5\big(m_B^2, \mu_\rho^2, m_{\tilde{l}_{L_2}}^2, m_{\tilde{l}_{L_2}}^2, m_{\tilde{l}_{R_2}}^2\big)\big) - c_L^2\big(J_5\big(m_B^2, \mu_\rho^2, \mu_\rho^2, m_{\tilde{l}_{L_3}}^2, m_{\tilde{l}_{R_2}}^2\big) \\
&+ J_5\big(m_B^2, \mu_\rho^2, m_{\tilde{l}_{L_3}}^2, m_{\tilde{l}_{L_3}}^2, m_{\tilde{l}_{R_2}}^2\big)\big)\big] - (R_2 \to R_3).
\end{aligned} \tag{C.4}
$$

Formulas for $A^{Z(c)}$:

$$
\begin{aligned}
A_L^{Z(c)} &= (s_L c_L) \times \frac{m_\tau^2 t^2 c_W^2}{16\pi^2\, V^2} \times \frac{1}{6}\big(t_\gamma^2 \mu_\rho^2\big)\big\{s_L^2\big[s_R^2 J_5\big(m_\lambda^2, m_{\tilde{l}_{R_2}}^2, m_{\tilde{l}_{R_2}}^2, m_{\tilde{l}_{L_2}}^2, m_{\tilde{l}_{L_2}}^2\big) \\
&+ c_R^2 J_5\big(m_\lambda^2, m_{\tilde{l}_{R_3}}^2, m_{\tilde{l}_{R_3}}^2, m_{\tilde{l}_{L_2}}^2, m_{\tilde{l}_{L_2}}^2\big)\big] \\
&- c_L^2\big[s_R^2 J_5\big(m_\lambda^2, m_{\tilde{l}_{R_2}}^2, m_{\tilde{l}_{R_2}}^2, m_{\tilde{l}_{L_3}}^2, m_{\tilde{l}_{L_3}}^2\big) + c_R^2 J_5\big(m_\lambda^2, m_{\tilde{l}_{R_3}}^2, m_{\tilde{l}_{R_3}}^2, m_{\tilde{l}_{L_3}}^2, m_{\tilde{l}_{L_3}}^2\big)\big] \\
&- \big(s_L^2 - c_L^2\big)\big[s_R^2 J_5\big(m_\lambda^2, m_{\tilde{l}_{R_2}}^2, m_{\tilde{l}_{R_2}}^2, m_{\tilde{l}_{L_2}}^2, m_{\tilde{l}_{L_3}}^2\big) \\
&+ c_R^2 J_5\big(m_\lambda^2, m_{\tilde{l}_{R_3}}^2, m_{\tilde{l}_{R_3}}^2, m_{\tilde{l}_{L_2}}^2, m_{\tilde{l}_{L_3}}^2\big)\big]\big\} \\
&+ (s_L c_L) \times \frac{m_\tau^2 t^2 c_W^2}{16\pi^2\, V^2} \times \frac{1}{108}\big(t_\gamma^2 \mu_\rho^2\big)\big\{s_L^2\big[s_R^2 J_5\big(m_B^2, m_{\tilde{l}_{R_2}}^2, m_{\tilde{l}_{R_2}}^2, m_{\tilde{l}_{L_2}}^2, m_{\tilde{l}_{L_2}}^2\big) \\
&+ c_R^2 J_5\big(m_B^2, m_{\tilde{l}_{R_3}}^2, m_{\tilde{l}_{R_3}}^2, m_{\tilde{l}_{L_2}}^2, m_{\tilde{l}_{L_2}}^2\big)\big] \\
&- c_L^2\big[s_R^2 J_5\big(m_B^2, m_{\tilde{l}_{R_2}}^2, m_{\tilde{l}_{R_2}}^2, m_{\tilde{l}_{L_3}}^2, m_{\tilde{l}_{L_3}}^2\big) + c_R^2 J_5\big(m_B^2, m_{\tilde{l}_{R_3}}^2, m_{\tilde{l}_{R_3}}^2, m_{\tilde{l}_{L_3}}^2, m_{\tilde{l}_{L_3}}^2\big)\big] \\
&- \big(s_L^2 - c_L^2\big)\big[s_R^2 J_5\big(m_B^2, m_{\tilde{l}_{R_2}}^2, m_{\tilde{l}_{R_2}}^2, m_{\tilde{l}_{L_2}}^2, m_{\tilde{l}_{L_3}}^2\big) \\
&+ c_R^2 J_5\big(m_B^2, m_{\tilde{l}_{R_3}}^2, m_{\tilde{l}_{R_3}}^2, m_{\tilde{l}_{L_2}}^2, m_{\tilde{l}_{L_3}}^2\big)\big]\big\},
\end{aligned} \tag{C.5}
$$

$$
\begin{aligned}
A_R^{Z(c)} &= (s_R c_R) \times \frac{m_\tau^2 t^2 c_W^2}{16\pi^2\, V^2} \times \frac{1}{12}\big(t_\gamma^2 \mu_\rho^2\big)\big\{-s_R^2\big[s_L^2 J_5\big(m_B^2, m_{\tilde{l}_{R_2}}^2, m_{\tilde{l}_{R_2}}^2, m_{\tilde{l}_{L_2}}^2, m_{\tilde{l}_{L_2}}^2\big) \\
&+ c_L^2 J_5\big(m_B^2, m_{\tilde{l}_{R_2}}^2, m_{\tilde{l}_{R_2}}^2, m_{\tilde{l}_{L_3}}^2, m_{\tilde{l}_{L_3}}^2\big)\big] \\
&+ c_R^2\big[s_L^2 J_5\big(m_B^2, m_{\tilde{l}_{R_3}}^2, m_{\tilde{l}_{R_3}}^2, m_{\tilde{l}_{L_2}}^2, m_{\tilde{l}_{L_2}}^2\big) + c_L^2 J_5\big(m_B^2, m_{\tilde{l}_{R_3}}^2, m_{\tilde{l}_{R_3}}^2, m_{\tilde{l}_{L_3}}^2, m_{\tilde{l}_{L_3}}^2\big)\big] \\
&+ \big(s_R^2 - c_R^2\big)\big[s_L^2 J_5\big(m_B^2, m_{\tilde{l}_{R_2}}^2, m_{\tilde{l}_{R_3}}^2, m_{\tilde{l}_{L_2}}^2, m_{\tilde{l}_{L_2}}^2\big) \\
&+ c_L^2 J_5\big(m_B^2, m_{\tilde{l}_{R_2}}^2, m_{\tilde{l}_{R_3}}^2, m_{\tilde{l}_{L_3}}^2, m_{\tilde{l}_{L_3}}^2\big)\big]\big\}.
\end{aligned} \tag{C.6}
$$

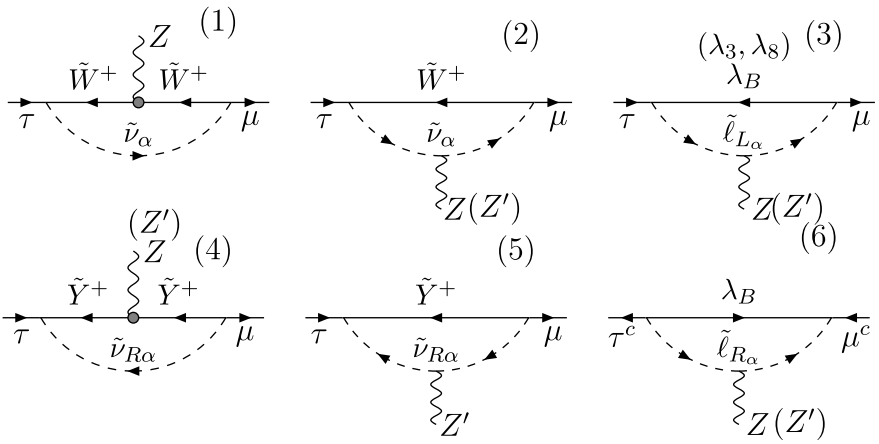

Fig. 16. Diagrams contributing to $C^Z_{L,R}$ ($C^{Z'}_{L,R}$). Only the last gives contribution to C^Z_R ($C^{Z'}_R$). The first diagram only contributes to C^Z_L while the fifth only contributes to $C^{Z'}_L$.

C.2. Contributions to $C^Z_{L,R}$

For $C^Z_{L,R}$, in Fig. 16. The formulas for these two quantities are written as below:

$$
\begin{aligned}
C^Z_L = {} & (c_{\nu_L} s_{\nu_L}) \times \frac{g^2}{16\pi^2} \times \frac{1}{12}\big[-K_5\big(m^2_\lambda, m^2_{\tilde{\nu}_{L2}}, m^2_{\tilde{\nu}_{L2}}, m^2_{\tilde{\nu}_{L2}}, m^2_{\tilde{\nu}_{L2}}\big)\big] \\
& + (c_L s_L) \times \frac{g^2}{16\pi^2} \times \frac{1}{18} c_{2W}\big[-K_5\big(m^2_\lambda, m^2_{\tilde{l}_{L2}}, m^2_{\tilde{l}_{L2}}, m^2_{\tilde{l}_{L2}}, m^2_{\tilde{l}_{L2}}\big)\big] \\
& + (c_{\nu_L} s_{\nu_L}) \times \frac{g^2}{16\pi^2} \times \frac{1}{12} c^2_{\tilde{W}}\big[-2K_5\big(m^2_\lambda, m^2_\lambda, m^2_\lambda, m^2_\lambda, \tilde{m}^2_{\nu_{L2}}\big) \\
& + 3m^2_\lambda J_5\big(m^2_\lambda, m^2_\lambda, m^2_\lambda, m^2_\lambda, \tilde{m}^2_{\nu_{L2}}\big)\big] \\
& + (c_{\nu_R} s_{\nu_R}) \times \frac{g^2}{16\pi^2} \times \frac{c_{2W}}{12}\big[-2K_5\big(m^2_\lambda, m^2_\lambda, m^2_\lambda, m^2_\lambda, \tilde{m}^2_{\nu_{R2}}\big) \\
& + 3m^2_\lambda J_5\big(m^2_\lambda, m^2_\lambda, m^2_\lambda, m^2_\lambda, \tilde{m}^2_{\nu_{R2}}\big)\big] \\
& + (c_L s_L) \times \frac{g'^2}{16\pi^2} \times \frac{1}{324}\big(1 - 2s^2_W\big)\big[K_5\big(m^2_B, m^2_{\tilde{l}_{L2}}, m^2_{\tilde{l}_{L2}}, m^2_{\tilde{l}_{L2}}, m^2_{\tilde{l}_{L2}}\big)\big] \\
& - [L_2 \to L_3,\ R_2 \to R_3], \qquad \text{(C.7)} \\
C^Z_R = {} & (c_R s_R) \times \frac{g'^2}{16\pi^2} \times \frac{1}{36} s^2_W\big[K_5\big(m^2_B, m^2_{\tilde{l}_{R2}}, m^2_{\tilde{l}_{R2}}, m^2_{\tilde{l}_{R2}}, m^2_{\tilde{l}_{R2}}\big)\big] \\
& - [R_2 \to R_3]. \qquad \text{(C.8)}
\end{aligned}
$$

We note that because Z boson couples much weakly to right-handed neutrinos so the diagram 5 in Fig. 16 give suppressed contribution to C^Z_L. In contrast, the case of Z' boson is different, it weakly couples with $\tilde{W}^\pm$ but non-negligible to right-handed neutrinos. So for the $C^{Z'}_L$, we neglect the first diagram and keep the fifth. This conclusion is held in the case of D^Z and $D^{Z'}$.

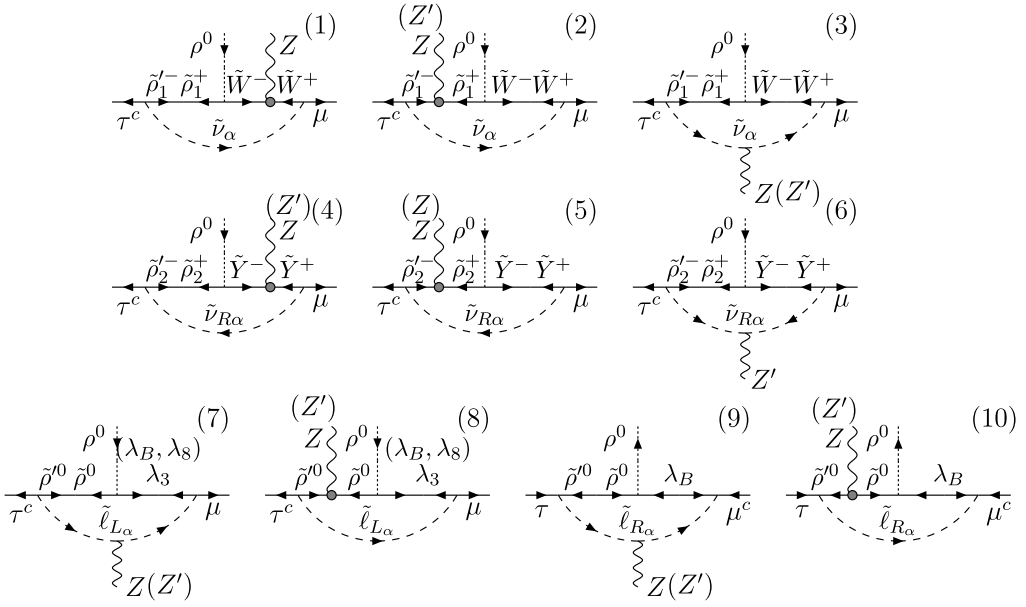

Fig. 17. Diagrams contributing to $D_L^{Z(b)}$ ($D_L^{Z'(b)}$) (two first lines) and $D_R^{Z(b)}$ ($D_R^{Z'(b)}$) (the last line). Noting that the first diagram only contributes to $D_L^{Z(b)}$ while the sixth only contributes to $D_L^{Z'(b)}$.

C.3. Contributions to $D_{L,R}^Z$

For $D_{L,R}^Z$, we have $D_{L,R}^Z = D_{L,R}^{Z(b)} + D_{L,R}^{Z(c)}$. They are presented by diagrams in Figs. 17 and 18. Formulas for $D^{Z(b)}$:

$$
\begin{aligned}
D_L^{Z(b)} &= (s_L c_L)\frac{g^2}{16\pi^2} \times \frac{1}{6} \times \mu_\rho m_\lambda \tan\gamma \\
&\quad \times \left[2J_5\left(m_\lambda^2, \mu_\rho^2, \mu_\rho^2, \mu_\rho^2, m_{\tilde{l}_{L2}}^2\right) + J_5\left(m_\lambda^2, m_\lambda^2, \mu_\rho^2, \mu_\rho^2, m_{\tilde{l}_{L2}}^2\right)\right] \\
&\quad + (s_L c_L)\frac{g^2}{16\pi^2} \times \frac{1}{3}\mu_\rho m_\lambda \tan\gamma c_{2W}\left[m_{\tilde{l}_{L2}}^2 I_5\left(m_\lambda^2, \mu_\rho^2, m_{\tilde{l}_{L2}}^2, m_{\tilde{l}_{L2}}^2, m_{\tilde{l}_{L2}}^2\right)\right] \\
&\quad + (s_{\nu_L} c_{\nu_L})\frac{g^2}{16\pi^2} \times \frac{1}{2}\mu_\rho m_\lambda \tan\gamma m_{\tilde{\nu}_{L2}}^2 I_5\left(m_\lambda^2, \mu_\rho^2, m_{\tilde{\nu}_{L2}}^2, m_{\tilde{\nu}_{L2}}^2, m_{\tilde{\nu}_{L2}}^2\right) \\
&\quad - (s_{\nu_L} c_{\nu_L})\frac{g^2}{16\pi^2} \times \frac{1}{2}(\mu_\rho m_\lambda \tan\gamma) \\
&\quad \times c_W^2\left[2J_5\left(m_\lambda^2, m_\lambda^2, m_\lambda^2, \mu_\rho^2, m_{\tilde{\nu}_{L2}}^2\right) + J_5\left(m_\lambda^2, m_\lambda^2, \mu_\rho^2, \mu_\rho^2, m_{\tilde{\nu}_{L2}}^2\right)\right] \\
&\quad - (s_{\nu_R} c_{\nu_R})\frac{g^2}{16\pi^2} \times \frac{1}{4}(\mu_\rho m_\lambda \tan\gamma) \\
&\quad \times c_{2W}\left[2J_5\left(m_\lambda^2, m_\lambda^2, m_\lambda^2, \mu_\rho^2, m_{\tilde{\nu}_{R2}}^2\right) + J_5\left(m_\lambda^2, m_\lambda^2, \mu_\rho^2, \mu_\rho^2, m_{\tilde{\nu}_{R2}}^2\right)\right] \\
&\quad + (s_{\nu_L} c_{\nu_L})\frac{g^2}{16\pi^2} \times (\mu_\rho m_\lambda \tan\gamma) \times \frac{1}{4} \\
&\quad \times \left(-1 + 2s_W^2\right)\left[2J_5\left(m_\lambda^2, \mu_\rho^2, \mu_\rho^2, \mu_\rho^2, m_{\tilde{\nu}_{L2}}^2\right) + J_5\left(m_\lambda^2, m_\lambda^2, \mu_\rho^2, \mu_\rho^2, m_{\tilde{\nu}_{L2}}^2\right)\right]
\end{aligned}
$$

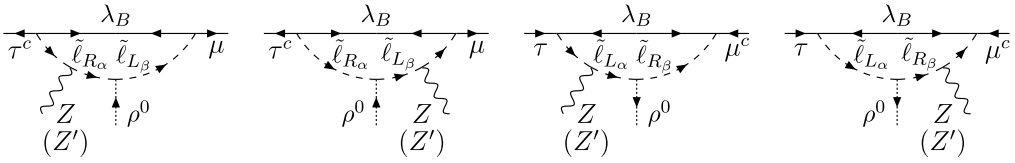

Fig. 18. Diagrams that contribute to $D_{L,R}^{Z(c)}$ ($D_{L,R}^{Z'(c)}$).

$$
\begin{aligned}
&+ (s_{\nu_R} c_{\nu_R}) \frac{g^2}{16\pi^2} \times (\mu_\rho m_\lambda \tan\gamma) \times \frac{1}{4} \\
&\times s_W^2 \big[2J_5\big(m_\lambda^2, \mu_\rho^2, \mu_\rho^2, \mu_\rho^2, m_{\tilde{\nu}_{R2}}^2\big) + J_5\big(m_\lambda^2, m_\lambda^2, \mu_\rho^2, \mu_\rho^2, m_{\tilde{\nu}_{R2}}^2\big) \big] \\
&+ (s_L c_L) \frac{g'^2}{16\pi^2} \times \frac{1}{27} \times \mu_\rho m_B \tan\gamma \\
&\times c_{2W} m_{\tilde{l}_{L2}}^2 I_5\big(m_B^2, \mu_\rho^2, m_{\tilde{l}_{L2}}^2, m_{\tilde{l}_{L2}}^2, m_{\tilde{l}_{L2}}^2\big) \\
&+ (s_L c_L) \frac{g'^2}{16\pi^2} \times \frac{1}{54} \times \mu_\rho m_B \tan\gamma \\
&\times \big[2J_5\big(m_B^2, \mu_\rho^2, \mu_\rho^2, \mu_\rho^2, m_{\tilde{l}_{L2}}^2\big) + J_5\big(m_B^2, m_B^2, \mu_\rho^2, \mu_\rho^2, m_{\tilde{l}_{L2}}^2\big) \big] \\
&- (L_2 \to L_3,\ R_2 \to R_3), \qquad \text{(C.9)}
\end{aligned}
$$

$$
\begin{aligned}
D_R^{Z(b)} = &-(s_R c_R) \frac{g'^2}{16\pi^2} \times \frac{1}{18} m_B \mu_\rho \tan\gamma \\
&\times \big[\big(-4s_W^2\big) m_{\tilde{l}_{R2}}^2 I_5\big(m_B^2, \mu_\rho^2, m_{\tilde{l}_{R2}}^2, m_{\tilde{l}_{R2}}^2, m_{\tilde{l}_{R2}}^2\big) \\
&+ 2J_5\big(m_B^2, \mu_\rho^2, \mu_\rho^2, \mu_\rho^2, m_{\tilde{l}_{R2}}^2\big) + J_5\big(m_B^2, m_B^2, \mu_\rho^2, \mu_\rho^2, m_{\tilde{l}_{R2}}^2\big) \big] \\
&- (R_2 \to R_3). \qquad \text{(C.10)}
\end{aligned}
$$

Formulas for $D_{L,R}^{Z(c)}$:

$$
\begin{aligned}
D_L^{Z(c)} = &-(s_L c_L) \frac{g'^2}{16\pi^2} m_B \mu_\rho \tan\gamma \times \frac{1}{72} \\
&\times \big[\big(1 - 2s_W^2\big) \big(s_R^2 J_5\big(m_B^2, m_B^2, m_{\tilde{l}_{L2}}^2, m_{\tilde{l}_{L2}}^2, m_{\tilde{l}_{R2}}^2\big) \\
&+ c_R^2 J_5\big(m_B^2, m_B^2, m_{\tilde{l}_{L2}}^2, m_{\tilde{l}_{L2}}^2, m_{\tilde{l}_{R3}}^2\big) \big) \\
&+ 2s_W^2 \big(s_R^2 J_5\big(m_B^2, m_B^2, m_{\tilde{l}_{L2}}^2, m_{\tilde{l}_{R2}}^2, m_{\tilde{l}_{R2}}^2\big) \\
&+ c_R^2 J_5\big(m_B^2, m_B^2, m_{\tilde{l}_{L2}}^2, m_{\tilde{l}_{R3}}^2, m_{\tilde{l}_{R3}}^2\big) \big) \big] - (L_2 \to L_3), \qquad \text{(C.11)}
\end{aligned}
$$

$$
\begin{aligned}
D_R^{Z(c)} = &-(s_R c_R) \times \frac{g'^2}{16\pi^2} m_B \mu_\rho \tan\gamma \times \frac{1}{72} \\
&\times \big[\big(1 - 2s_W^2\big) \big(s_L^2 J_5\big(m_B^2, m_B^2, m_{\tilde{l}_{L2}}^2, m_{\tilde{l}_{L2}}^2, m_{\tilde{l}_{R2}}^2\big) \\
&+ c_L^2 J_5\big(m_B^2, m_B^2, m_{\tilde{l}_{L3}}^2, m_{\tilde{l}_{L3}}^2, m_{\tilde{l}_{R2}}^2\big) \big) \\
&+ 2s_W^2 \big(s_L^2 J_5\big(m_B^2, m_B^2, m_{\tilde{l}_{L2}}^2, m_{\tilde{l}_{R2}}^2, m_{\tilde{l}_{R2}}^2\big) \\
&+ c_L^2 J_5\big(m_B^2, m_B^2, m_{\tilde{l}_{L3}}^2, m_{\tilde{l}_{R2}}^2, m_{\tilde{l}_{R2}}^2\big) \big) \big] - (R_2 \to R_3). \qquad \text{(C.12)}
\end{aligned}
$$

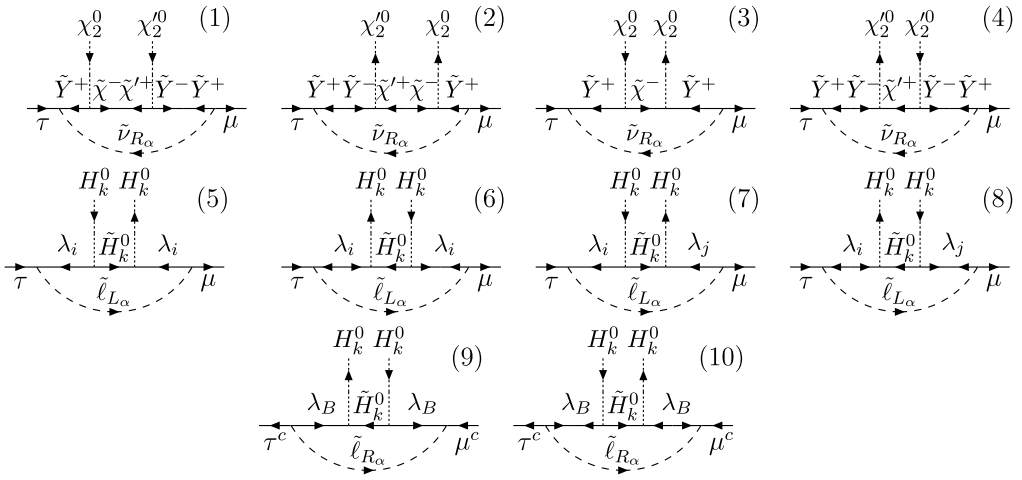

Fig. 19. Diagrams contributing to $A_L^{(2Z')}$ (first and second rows) and $A_R^{(2Z')}$ (third row). Here we denote $H_k^0 \in \{\chi_2^0, \chi_2'^0\}$ while $\lambda_{i,j}$ implies $i, j = \{B, 8\}$ and $i \neq j$.

Appendix D. Contributions to $Z' \to \mu\tau$

D.1. Contributions to $A_{L,R}^{1Z'}$

To determine the values of $A_{L,R}^{Z}$, $A_{L,R}^{1Z'}$ and $A_{L,R}^{2Z'}$, we use techniques mentioned in [10]. From formulas of covariant derivatives of neutral Higgs in Appendix A.2, it is easy to see that two terms relating with Z and Z' bosons appearing in these covariant derivatives are different from each others one factor (-1). For $A_{L,R}^{1Z'}$ which relates with ρ^0 and ρ'^0 we have $A_{L,R}^{1Z'} = A_{L,R}^{1Z'(a)} + A_{L,R}^{Z'(b)} + A_{L,R}^{Z'(c)}$ and $A_{L(R)}^{Z'} = (m_Z^2/m_{Z'}^2)A_{L(R)}^{1Z'} + A_{L(R)}^{2Z'}$. This leads to the results:

$$\begin{aligned} A_{L,R}^{1Z'(a)} &= -A_{L,R}^{Z(a)}, \\ A_{L,R}^{Z'(b)} &= -A_{L,R}^{Z(b)}, \\ A_{L,R}^{Z'(c)} &= -A_{L,R}^{Z(c)}. \end{aligned} \tag{D.1}$$

D.2. Contributions to $A_{L,R}^{2Z'}$

Diagrams contributing to $A_{L,R}^{2Z'}$ are quite similar to those shown in Fig. 14. There is a interesting point in the SUSYE331 model that both Higgs χ and χ' do not couple to leptons and sleptons. As a consequence, $A_{L,R}^{(2Z')}$ give contributions from only the class of diagrams depicted in Fig. 19 where ρ^0, ρ'^0 and Z boson in Fig. 14 are correspondingly replaced with χ_2^0, χ_2^0 and Z' boson. We use the equivalence role between $\rho^0 \leftrightarrow \chi_2^0$ and $\rho'^0 \leftrightarrow \chi_2'^0$ for the calculation (see Appendix A.2). The results are:

$$A_L^{(2Z')} = (s_{\nu_R} c_{\nu_R}) \frac{g^2 \kappa_1^2}{16\pi^2} \times \frac{1}{4} m_\lambda \mu_\chi s_{2\beta} J_5\big(m_\lambda^2, m_\lambda^2, \mu_\chi^2, \mu_\chi^2, \tilde{m}_{\tilde{\nu}_{R2}}^2\big)$$

$$
\begin{aligned}
&- (s_{\nu_R} c_{\nu_R}) \frac{g^2 \kappa_1^2}{16\pi^2} \times \frac{1}{4} s_\beta^2 \big[2 J_4\big(m_\lambda^2, m_\lambda^2, \mu_\chi^2, \tilde{m}^2_{\tilde{\nu}_{R2}}\big) \\
&+ \mu_\chi^2 J_5\big(m_\lambda^2, m_\lambda^2, \mu_\chi^2, \mu_\chi^2, \tilde{m}^2_{\tilde{\nu}_{R2}}\big)\big] \\
&- (s_{\nu_R} c_{\nu_R}) \frac{g^2 \kappa_1^2}{16\pi^2} \times \frac{1}{4} m_\lambda^2 c_\beta^2 \big[\mu_\chi^2 I_5\big(m_\lambda^2, m_\lambda^2, \mu_\chi^2, \mu_\chi^2, \tilde{m}^2_{\tilde{\nu}_{R2}}\big) \\
&- I_4\big(m_\lambda^2, m_\lambda^2, \mu_\chi^2, \tilde{m}^2_{\tilde{\nu}_{R2}}\big)\big] \\
&+ (s_L c_L) \frac{g'^2 t^2 \kappa_1^2}{16\pi^2} \times \frac{1}{2916} c_{2\beta} \big[2 J_4\big(m_B^2, m_B^2, \mu_\chi^2, \tilde{m}^2_{\tilde{\ell}_{L2}}\big) \\
&+ \mu_\chi^2 J_5\big(m_B^2, m_B^2, \mu_\chi^2, \mu_\chi^2, \tilde{m}^2_{\tilde{\ell}_{L2}}\big)\big] \\
&+ (s_L c_L) \frac{g^2 \kappa_1^2}{16\pi^2} \times \frac{1}{9} c_{2\beta} \big[2 J_4\big(m_\lambda^2, m_\lambda^2, \mu_\chi^2, \tilde{m}^2_{\tilde{\ell}_{L2}}\big) \\
&+ \mu_\chi^2 J_5\big(m_\lambda^2, m_\lambda^2, \mu_\chi^2, \mu_\chi^2, \tilde{m}^2_{\tilde{\ell}_{L2}}\big)\big] \\
&- (s_L c_L) \frac{g'^2 t^2 \kappa_1^2}{16\pi^2} \times \frac{1}{2916} m_B^2 c_{2\beta} \big[\mu_\chi^2 I_5\big(m_B^2, m_B^2, \mu_\chi^2, \mu_\chi^2, \tilde{m}^2_{\tilde{\ell}_{L2}}\big) \\
&- I_4\big(m_B^2, m_B^2, \mu_\chi^2, \tilde{m}^2_{\tilde{\ell}_{L2}}\big)\big] \\
&- (s_L c_L) \frac{g^2 \kappa_1^2}{16\pi^2} \times \frac{1}{9} m_\lambda^2 c_{2\beta} \big[\mu_\chi^2 I_5\big(m_\lambda^2, m_\lambda^2, \mu_\chi^2, \mu_\chi^2, \tilde{m}^2_{\tilde{\ell}_{L2}}\big) \\
&- I_4\big(m_\lambda^2, m_\lambda^2, \mu_\chi^2, \tilde{m}^2_{\tilde{\ell}_{L2}}\big)\big] \\
&- (s_L c_L) \frac{g'^2 \kappa_1^2}{16\pi^2} \times \frac{1}{162} c_{2\beta} \big[2 J_4\big(m_B^2, m_\lambda^2, \mu_\chi^2, \tilde{m}^2_{\tilde{\ell}_{L2}}\big) \\
&+ \mu_\chi^2 J_5\big(m_B^2, m_\lambda^2, \mu_\chi^2, \mu_\chi^2, \tilde{m}^2_{\tilde{\ell}_{L2}}\big)\big] \\
&+ (s_L c_L) \frac{g'^2 \kappa_1^2}{16\pi^2} \times \frac{1}{162} m_B m_\lambda c_{2\beta} \big[\mu_\chi^2 I_5\big(m_B^2, m_\lambda^2, \mu_\chi^2, \mu_\chi^2, \tilde{m}^2_{\tilde{\ell}_{L2}}\big) \\
&- I_4\big(m_B^2, m_\lambda^2, \mu_\chi^2, \tilde{m}^2_{\tilde{\ell}_{L2}}\big)\big] \\
&- (L_2 \to L_3, R_2 \to R_3), \qquad \text{(D.2)}
\end{aligned}
$$

$$
\begin{aligned}
A_R^{(2Z')} = &- (s_R c_R) \frac{g'^2 t^2 \kappa_1^2}{16\pi^2} \times \frac{1}{324} c_{2\beta} \big[2 J_4\big(m_B^2, m_B^2, \mu_\chi^2, \tilde{m}^2_{\tilde{\ell}_{R2}}\big) \\
&+ \mu_\chi^2 J_5\big(m_B^2, m_B^2, \mu_\chi^2, \mu_\chi^2, \tilde{m}^2_{\tilde{\ell}_{R2}}\big)\big] \\
&+ (s_R c_R) \frac{g'^2 \kappa_1^2}{16\pi^2} \times \frac{1}{324} m_B^2 c_{2\beta} \big[\mu_\chi^2 I_5\big(m_B^2, m_B^2, \mu_\chi^2, \mu_\chi^2, \tilde{m}^2_{\tilde{\ell}_{R2}}\big) \\
&- I_4\big(m_B^2, m_B^2, \mu_\chi^2, \tilde{m}^2_{\tilde{\ell}_{R2}}\big)\big] \\
&- (R_2 \to R_3). \qquad \text{(D.3)}
\end{aligned}
$$

D.3. Contributions to $C^{Z'}_{L,R}$

Diagrams contributing to $C^{Z'}_{L,R}$ are those from 2–6 in Fig. 16. Comparing with the case of the Z boson we easily deduce the formulas as:

$$
\begin{aligned}
C_L^{Z'} = &-(c_{\nu_L} s_{\nu_L}) \times \frac{g^2}{16\pi^2} \times \frac{1}{12} c_{2W} \big[K_5\big(m_\lambda^2, m_{\tilde{\nu}_{L2}}^2, m_{\tilde{\nu}_{L2}}^2, m_{\tilde{\nu}_{L2}}^2, m_{\tilde{\nu}_{L2}}^2\big)\big] \\
&- (c_L s_L) \times \frac{g^2}{16\pi^2} \times \frac{1}{18} c_{2W} \big[-K_5\big(m_\lambda^2, m_{\tilde{l}_{L2}}^2, m_{\tilde{l}_{L2}}^2, m_{\tilde{l}_{L2}}^2, m_{\tilde{l}_{L2}}^2\big)\big] \\
&- (c_{\nu_R} s_{\nu_R}) \times \frac{g^2}{16\pi^2} \times \frac{4c_W^2 - 1}{12} \big[-2K_5\big(m_\lambda^2, m_\lambda^2, m_\lambda^2, m_\lambda^2, \tilde{m}_{\nu_{R2}}^2\big) \\
&+ 3m_\lambda^2 J_5\big(m_\lambda^2, m_\lambda^2, m_\lambda^2, m_\lambda^2, \tilde{m}_{\nu_{R2}}^2\big)\big] \\
&+ (c_L s_L) \times \frac{g'^2}{16\pi^2} \times \frac{1}{324}\big(1 - 2s_W^2\big)\big[K_5\big(m_B^2, m_{\tilde{l}_{L2}}^2, m_{\tilde{l}_{L2}}^2, m_{\tilde{l}_{L2}}^2, m_{\tilde{l}_{L2}}^2\big)\big] \\
&+ (c_{\nu_R} s_{\nu_R}) \times \frac{g^2}{16\pi^2} \times \frac{1}{12} c_W^2 \big[K_5\big(m_\lambda^2, m_{\tilde{\nu}_{R2}}^2, m_{\tilde{\nu}_{R2}}^2, m_{\tilde{\nu}_{R2}}^2, m_{\tilde{\nu}_{R2}}^2\big)\big] \\
&- (L_2 \to L_3), \qquad \text{(D.4)} \\
C_R^{Z'} = &-C_R^Z. \qquad \text{(D.5)}
\end{aligned}
$$

D.4. Contributions to $D_{L,R}^{Z'}$

Contribution to $D_{L,R}^{Z'}$ can be deduced from diagrams shown for $D_{L,R}^{Z}$ in Figs. 17 and 18. We also write $D_{L,R}^{Z'} = D_{L,R}^{Z'(b)} + D_{L,R}^{Z'(c)}$. From Fig. 17 we can deduce formulas to determine $D^{Z'(b)}$:

$$
\begin{aligned}
D_L^{Z'(b)} = &-(s_{\nu_L} c_{\nu_L}) \frac{g^2}{16\pi^2} \times (\mu_\rho m_\lambda \tan\gamma) \times \frac{1}{4} \\
&\times \big[2J_5\big(m_\lambda^2, \mu_\rho^2, \mu_\rho^2, \mu_\rho^2, m_{\tilde{\nu}_{L2}}^2\big) + J_5\big(m_\lambda^2, m_\lambda^2, \mu_\rho^2, \mu_\rho^2, m_{\tilde{\nu}_{L2}}^2\big)\big] \\
&+ (s_{\nu_L} c_{\nu_L}) \frac{g^2}{16\pi^2} \times \frac{1}{2} \mu_\rho m_\lambda \tan\gamma \\
&\times c_{2W} \big[m_{\tilde{\nu}_{L2}}^2 I_5\big(m_\lambda^2, \mu_\rho^2, m_{\tilde{\nu}_{L2}}^2, m_{\tilde{\nu}_{L2}}^2, m_{\tilde{\nu}_{L2}}^2\big)\big] \\
&+ (s_{\nu_R} c_{\nu_R}) \frac{g^2}{16\pi^2} \times \frac{1}{4} (\mu_\rho m_\lambda \tan\gamma) \\
&\times \kappa_1^2 \big[2J_5\big(m_\lambda^2, m_\lambda^2, m_\lambda^2, \mu_\rho^2, m_{\tilde{\nu}_{R2}}^2\big) + J_5\big(m_\lambda^2, m_\lambda^2, \mu_\rho^2, \mu_\rho^2, m_{\tilde{\nu}_{R2}}^2\big)\big] \\
&+ (s_{\nu_R} c_{\nu_R}) \frac{g^2}{16\pi^2} \times (\mu_\rho m_\lambda \tan\gamma) \times \frac{1}{4} \\
&\times c_{2W} \big[2J_5\big(m_\lambda^2, \mu_\rho^2, \mu_\rho^2, \mu_\rho^2, m_{\tilde{\nu}_{R2}}^2\big) + J_5\big(m_\lambda^2, m_\lambda^2, \mu_\rho^2, \mu_\rho^2, m_{\tilde{\nu}_{R2}}^2\big)\big] \\
&+ (s_{\nu_R} c_{\nu_R}) \frac{g^2}{16\pi^2} \times \mu_\rho m_\lambda \tan\gamma \\
&\times c_W^2 \big[m_{\tilde{\nu}_{R2}}^2 I_5\big(m_\lambda^2, \mu_\rho^2, m_{\tilde{\nu}_{R2}}^2, m_{\tilde{\nu}_{R2}}^2, m_{\tilde{\nu}_{R2}}^2\big)\big] \\
&- (s_L c_L) \frac{g'^2}{16\pi^2} \times \frac{1}{27} \times \mu_\rho m_B \tan\gamma \\
&\times c_{2W} \big[m_{\tilde{l}_{L2}}^2 I_5\big(m_B^2, \mu_\rho^2, m_{\tilde{l}_{L2}}^2, m_{\tilde{l}_{L2}}^2, m_{\tilde{l}_{L2}}^2\big)\big] \\
&- (s_L c_L) \frac{g^2}{16\pi^2} \times \frac{1}{3} \mu_\rho m_\lambda \tan\gamma \\
&\times c_{2W} \big[m_{\tilde{l}_{L2}}^2 I_5\big(m_\lambda^2, \mu_\rho^2, m_{\tilde{l}_{L2}}^2, m_{\tilde{l}_{L2}}^2, m_{\tilde{l}_{L2}}^2\big)\big]
\end{aligned}
$$

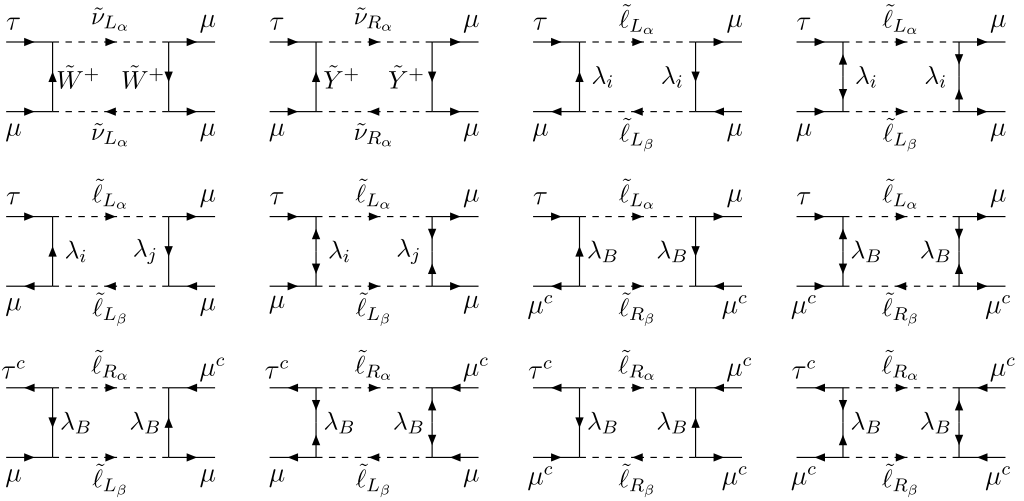

Fig. 20. Diagrams contributing to $B_L^{\mu_{L,R}}$ (first and second rows) and $B_R^{\mu_{L,R}}$ (third row). λ_i and λ_j ($i \neq j$ in each above diagram) are gauginos in which λ_i and $\lambda_j \in \{\lambda_B, \lambda_3, \lambda_8\}$.

$$
\begin{aligned}
&- (s_L c_L)\frac{g'^2}{16\pi^2} \times \frac{1}{54} \times \mu_\rho m_B \tan\gamma \\
&\times \left[2J_5\big(m_B^2, \mu_\rho^2, \mu_\rho^2, \mu_\rho^2, m_{\tilde{l}_{L2}}^2\big) + J_5\big(m_B^2, m_B^2, \mu_\rho^2, \mu_\rho^2, m_{\tilde{l}_{L2}}^2\big)\right] \\
&- (s_L c_L)\frac{g^2}{16\pi^2} \times \frac{1}{6} \times \mu_\rho m_\lambda \tan\gamma \\
&\times \left[2J_5\big(m_\lambda^2, \mu_\rho^2, \mu_\rho^2, \mu_\rho^2, m_{\tilde{l}_{L2}}^2\big) + J_5\big(m_\lambda^2, m_\lambda^2, \mu_\rho^2, \mu_\rho^2, m_{\tilde{l}_{L2}}^2\big)\right] \\
&- (L_2 \to L_3,\ R_2 \to R_3),
\end{aligned} \tag{D.6}
$$

$$
D_R^{Z'(b)} = -D_R^{Z(b)}, \tag{D.7}
$$

$$
D_L^{Z'(c)} = -D_L^{Z(c)}, \tag{D.8}
$$

$$
D_R^{Z'(c)} = -D_R^{Z(c)}. \tag{D.9}
$$

Appendix E. Contribution from $B_{L,R}^{\mu_{L,R}}$ to $\tau \to 3\mu$

Contributions to $B_{L,R}^{\mu_{L,R}}$ arise from the diagrams in Fig. 20. The formulas are:

$$
\begin{aligned}
B_L^{\mu_L} = {} & (s_{\nu_L} c_{\nu_L}) \times \frac{g^4}{16\pi^2} \times \frac{1}{8}\Big[-c_{\nu_L}^2 J_4\big(m_\lambda^2, m_\lambda^2, m_{\tilde{\nu}_{L2}}^2, m_{\tilde{\nu}_{L2}}^2\big) \\
&+ s_{\nu_L}^2 J_4\big(m_\lambda^2, m_\lambda^2, m_{\tilde{\nu}_{L3}}^2, m_{\tilde{\nu}_{L3}}^2\big) + \big(c_{\nu_L}^2 - s_{\nu_L}^2\big) J_4\big(m_\lambda^2, m_\lambda^2, m_{\tilde{\nu}_{L2}}^2, m_{\tilde{\nu}_{L3}}^2\big)\Big] \\
&+ (s_{\nu_R} c_{\nu_R}) \frac{g^4}{16\pi^2} \times \frac{1}{8}\Big[-c_{\nu_R}^2 J_4\big(m_\lambda^2, m_\lambda^2, m_{\tilde{\nu}_{R2}}^2, m_{\tilde{\nu}_{R2}}^2\big) \\
&+ s_{\nu_R}^2 J_4\big(m_\lambda^2, m_\lambda^2, m_{\tilde{\nu}_{R3}}^2, m_{\tilde{\nu}_{R3}}^2\big) \\
&+ \big(c_{\nu_R}^2 - s_{\nu_R}^2\big) J_4\big(m_\lambda^2, m_\lambda^2, m_{\tilde{\nu}_{R2}}^2, m_{\tilde{\nu}_{R3}}^2\big)\Big]
\end{aligned}
$$

$$
\begin{aligned}
&+ (s_L c_L) \times \frac{g^4}{16\pi^2} \times \frac{1}{18} \\
&\times \Big[-c_L^2 \big(J_4\big(m_\lambda^2, m_\lambda^2, m_{\tilde{l}_{L2}}^2, m_{\tilde{l}_{L2}}^2\big) + 2m_\lambda^2 I_4\big(m_\lambda^2, m_\lambda^2, m_{\tilde{l}_{L2}}^2, m_{\tilde{l}_{L2}}^2\big) \big) \\
&+ s_L^2 \big(J_4\big(m_\lambda^2, m_\lambda^2, m_{\tilde{l}_{L3}}^2, m_{\tilde{l}_{L3}}^2\big) + 2m_\lambda^2 I_4\big(m_\lambda^2, m_\lambda^2, m_{\tilde{l}_{L3}}^2, m_{\tilde{l}_{L3}}^2\big) \big) \\
&+ \big(c_L^2 - s_L^2\big) \big(J_4\big(m_\lambda^2, m_\lambda^2, m_{\tilde{l}_{L2}}^2, m_{\tilde{l}_{L3}}^2\big) + 2m_\lambda^2 I_4\big(m_\lambda^2, m_\lambda^2, m_{\tilde{l}_{L2}}^2, m_{\tilde{l}_{L3}}^2\big) \big) \Big] \\
&+ (s_L c_L) \times \frac{g^2 g'^2}{16\pi^2} \times \frac{1}{162} \\
&\times \Big[-c_L^2 \big(J_4\big(m_B^2, m_\lambda^2, m_{\tilde{l}_{L2}}^2, m_{\tilde{l}_{L2}}^2\big) + 2m_B m_\lambda I_4\big(m_B^2, m_\lambda^2, m_{\tilde{l}_{L2}}^2, m_{\tilde{l}_{L2}}^2\big) \big) \\
&+ s_L^2 \big(J_4\big(m_B^2, m_\lambda^2, m_{\tilde{l}_{L3}}^2, m_{\tilde{l}_{L3}}^2\big) + 2m_B m_\lambda I_4\big(m_B^2, m_\lambda^2, m_{\tilde{l}_{L3}}^2, m_{\tilde{l}_{L3}}^2\big) \big) \\
&+ \big(c_L^2 - s_L^2\big) \big(J_4\big(m_B^2, m_\lambda^2, m_{\tilde{l}_{L2}}^2, m_{\tilde{l}_{L3}}^2\big) + 2m_B m_\lambda I_4\big(m_B^2, m_\lambda^2, m_{\tilde{l}_{L2}}^2, m_{\tilde{l}_{L3}}^2\big) \big) \Big] \\
&+ (s_L c_L) \times \frac{g'^4}{16\pi^2} \times \frac{1}{216} \\
&\times \Big[-c_L^2 \big(J_4\big(m_B^2, m_B^2, m_{\tilde{l}_{L2}}^2, m_{\tilde{l}_{L2}}^2\big) + 2m_B^2 I_4\big(m_B^2, m_B^2, m_{\tilde{l}_{L2}}^2, m_{\tilde{l}_{L2}}^2\big) \big) \\
&+ s_L^2 \big(J_4\big(m_B^2, m_B^2, m_{\tilde{l}_{L3}}^2, m_{\tilde{l}_{L3}}^2\big) + 2m_B^2 I_4\big(m_B^2, m_B^2, m_{\tilde{l}_{L3}}^2, m_{\tilde{l}_{L3}}^2\big) \big) \\
&+ \big(c_L^2 - s_L^2\big) \big(J_4\big(m_B^2, m_B^2, m_{\tilde{l}_{L2}}^2, m_{\tilde{l}_{L3}}^2\big) + 2m_B^2 I_4\big(m_B^2, m_B^2, m_{\tilde{l}_{L2}}^2, m_{\tilde{l}_{L3}}^2\big) \big) \Big], \qquad \text{(E.1)}
\end{aligned}
$$

$$
\begin{aligned}
\frac{B_L^{\mu_R}}{s_L c_L} &= \frac{g'^4}{16\pi^2} \times \frac{1}{648} \Big[c_R^2 \big(J_4\big(m_B^2, m_B^2, m_{\tilde{l}_{R2}}^2, m_{\tilde{l}_{L2}}^2\big) + 2m_B^2 I_4\big(m_B^2, m_B^2, m_{\tilde{l}_{R2}}^2, m_{\tilde{l}_{L2}}^2\big) \big) \\
&+ s_R^2 \big(J_4\big(m_B^2, m_B^2, m_{\tilde{l}_{R3}}^2, m_{\tilde{l}_{L2}}^2\big) + 2m_B^2 I_4\big(m_B^2, m_B^2, m_{\tilde{l}_{R3}}^2, m_{\tilde{l}_{L2}}^2\big) \big) \Big] \\
&- (L_2 \to L_3), \qquad \text{(E.2)} \\
\frac{B_R^{\mu_L}}{s_R c_R} &= \frac{g'^4}{16\pi^2} \times \frac{1}{648} \Big[c_L^2 \big(J_4\big(m_B^2, m_B^2, m_{\tilde{l}_{L2}}^2, m_{\tilde{l}_{R2}}^2\big) + 2m_B^2 I_4\big(m_B^2, m_B^2, m_{\tilde{l}_{L2}}^2, m_{\tilde{l}_{R2}}^2\big) \big) \\
&+ s_L^2 \big(J_4\big(m_B^2, m_B^2, m_{\tilde{l}_{L3}}^2, m_{\tilde{l}_{R2}}^2\big) + 2m_B^2 I_4\big(m_B^2, m_B^2, m_{\tilde{l}_{L3}}^2, m_{\tilde{l}_{R2}}^2\big) \big) \Big] \\
&- (R_2 \to R_3), \qquad \text{(E.3)} \\
\frac{B_R^{\mu_R}}{s_R c_R} &= \frac{g'^4}{16\pi^2} \times \frac{1}{18} \Big[-c_R^2 \big(J_4\big(m_B^2, m_B^2, m_{\tilde{l}_{R2}}^2, m_{\tilde{l}_{R2}}^2\big) + 2m_B^2 I_4\big(m_B^2, m_B^2, m_{\tilde{l}_{R2}}^2, m_{\tilde{l}_{R2}}^2\big) \big) \\
&+ s_R^2 \big(J_4\big(m_B^2, m_B^2, m_{\tilde{l}_{R3}}^2, m_{\tilde{l}_{R3}}^2\big) + 2m_B^2 I_4\big(m_B^2, m_B^2, m_{\tilde{l}_{R3}}^2, m_{\tilde{l}_{R3}}^2\big) \big) \\
&+ \big(c_R^2 - s_R^2\big) \big(J_4\big(m_B^2, m_B^2, m_{\tilde{l}_{R2}}^2, m_{\tilde{l}_{R3}}^2\big) + 2m_B^2 I_4\big(m_B^2, m_B^2, m_{\tilde{l}_{R2}}^2, m_{\tilde{l}_{R3}}^2\big) \big) \Big]. \qquad \text{(E.4)}
\end{aligned}
$$

References

[1] Belle Collaboration, Phys. Lett. B 687 (2010) 139.
[2] B. Aubert, et al., BABAR Collaboration, Phys. Rev. Lett. 104 (2010) 021802.
[3] P. Abreu, et al., DELPHI Collaboration, Z. Phys. C 73 (1997) 243.
[4] J. Beringer, et al., Particle Data Group, Phys. Rev. D 86 (2012) 010001.
[5] Y. Fukuda, et al., Phys. Rev. Lett. 81 (1998) 1562;
S. Fukuda, et al., Super-Kamiokande Collaboration, Phys. Rev. Lett. 85 (2000) 3999.

[6] J.A. Aguilar-Saavedra, et al., ECFA/DESY LC Physics Working Group Collaboration, arXiv:hep-ph/0106315.
[7] I-Hsiu Lee, Phys. Lett. B 138 (1984) 121;
I-Hsiu Lee, Nucl. Phys. B 246 (1984) 120.
[8] Jose I. Illana, Nucl. Phys. B (Proc. Suppl.) 116 (2003) 321;
E.O. Iltan, Eur. Phys. J. C 56 (2008) 113.
[9] Xiao-Jun Bi, Yuan-Ben Dai, Xiao-Yuan Qi, Phys. Rev. D 63 (2001) 096008.
[10] A. Brignole, A. Rossi, Nucl. Phys. B 701 (2004) 3–53, arXiv:hep-ph/0404211.
[11] K.S. Babu, C. Kolda, Phys. Rev. Lett. 89 (2002) 241802, arXiv:hep-ph/0206310;
Asmaa Abada, Debottam Das, Cédric Weiland, JHEP 1203 (2012) 100;
Asmaa Abada, Debottam Das, Avelino Vicent, Cedric Weiland, JHEP 1209 (2012) 015.
[12] H.K. Dreiner, H.E. Haberand, S.P. Martin, Phys. Rep. 494 (2010) 1, arXiv:0812.1594 [hep-ph];
S.P. Martin, A supersymmetry primer, arXiv:hep-ph/9709356.
[13] F. Pisano, V. Pleitez, Phys. Rev. D 46 (1992) 410;
P.H. Frampton, Phys. Rev. Lett. 69 (1992) 2889;
R. Foot, O.F. Hernandez, F. Pisano, V. Pleitez, Phys. Rev. D 47 (1993) 4158.
[14] M. Singer, J.W.F. Valle, J. Schechter, Phys. Rev. D 22 (1980) 738;
R. Foot, H.N. Long, Tuan A. Tran, Phys. Rev. D 50 (1994) 34(R), arXiv:hep-ph/9402243;
J.C. Montero, F. Pisano, V. Pleitez, Phys. Rev. D 47 (1993) 2918;
H.N. Long, Phys. Rev. D 54 (1996) 4691;
H.N. Long, Phys. Rev. D 53 (1996) 437;
H.N. Long, Mod. Phys. Lett. A 13 (1998) 1865.
[15] F. Pisano, Mod. Phys. Lett. A 11 (1996) 2639;
A. Doff, F. Pisano, Mod. Phys. Lett. A 14 (1999) 1133;
C.A. de, S. Pires, O.P. Ravinez, Phys. Rev. D 58 (1998) 035008;
C.A. de, S. Pires, Phys. Rev. D 60 (1999) 075013;
P.V. Dong, H.N. Long, Int. J. Mod. Phys. A 21 (2006) 6677.
[16] W.A. Ponce, Y. Giraldo, L.A. Sanchez, Phys. Rev. D 67 (2003) 075001.
[17] P.V. Dong, H.N. Long, D.T. Nhung, D.V. Soa, Phys. Rev. D 73 (2006) 035004;
P.V. Dong, D.T. Huong, Tr.T. Huong, H.N. Long, Phys. Rev. D 74 (2006) 053003;
P.V. Dong, H.T. Hung, H.N. Long, Phys. Rev. D 86 (2012) 033002;
For a review, see: P.V. Dong, H.N. Long, Adv. High Energy Phys. 2008 (2008) 739492, arXiv:0804.3239.
[18] J.G. Ferreira Jr., P.R.D. Pinheiro, C.A. de, S. Pires, P.S. Rodrigues da Silva, Phys. Rev. D 84 (2011) 095019;
V.N. Huyen, et al., Neutral currents in reduced minimal 3-3-1 model, arXiv:1210.5833, 2012.
[19] D.T. Huong, L.T. Hue, M.C. Rodriguez, H.N. Long, Nucl. Phys. B 870 (2013) 293, arXiv:1210.6776.
[20] P.V. Dong, D.T. Huong, M.C. Rodriguez, H.N. Long, Nucl. Phys. B 772 (2007) 150, arXiv:hep-ph/0701137;
D.T. Huong, H.N. Long, JHEP 0807 (2008) 049, arXiv:0804.3875 [hep-ph].
[21] P.T. Giang, L.T. Hue, D.T. Huong, H.N. Long, Nucl. Phys. B 864 (2012) 85.
[22] T.P. Cheng, L.F. Li, Gauge Theory of Elementary Particle Physics, Clarendon Press, Oxford, 1984.
[23] Benjamin W. Lee, Robert E. Shrock, Phys. Rev. D 16 (1977) 1444;
B.W. Lee, S. Pakvasa, R.E. Shrock, H. Sugawara, Phys. Rev. Lett. 38 (1977) 937.
[24] J. Hisano, T. Moroi, K. Kobe, M. Yamaguchi, Phys. Rev. D 53 (1996).
[25] A.I. Davydychev, J. Math. Phys. 32 (1991) 1052.
[26] P.V. Dong, D.T. Huong, N.T. Thuy, H.N. Long, Nucl. Phys. B 795 (2008) 361, arXiv:0707.3712 [hep-ph].
[27] P.V. Dong, Tr.T. Huong, N.T. Thuy, H.N. Long, JHEP 0711 (2007) 073, arXiv:0708.3155 [hep-ph].
[28] J.N. Esteves, J.C. Romario, M. Hirsch, A. Vicente, W. Porod, F. Staub, JHEP 1012 (2010) 077;
A. Abada, D. Das, A. Vicente, C. Weiland, JHEP 1209 (2012) 015.
[29] Stephen P. Martin, arXiv:hep-ph/9709356.
[30] G. Abbiendi, et al., ALEPH Collaboration, DELPHI Collaboration, L3 Collaboration, OPAL Collaboration, The LEP Working Group for Higgs Boson Searches, Search for charged Higgs bosons: Combined results using LEP data, arXiv:1301.6065 [hep-ex].
[31] L.T. Hue, D.T. Huong, H.N. Long, in preparation.